NASA TECHNICAL REPORT

NASA TR R-224

NASA TR R-224

GPO PRICE $ ________

CFSTI PRICE(S) $ 2.00

Hard copy (HC) ________

Microfiche (MF) .50

N65-28674 (ACCESSION NUMBER)	(THRU)
49 (PAGES)	1 (CODE)
(NASA CR OR TMX OR AD NUMBER)	33 (CATEGORY)

FACILITY FORM 602

CONVECTIVE HEAT TRANSFER IN PLANETARY GASES

by Joseph G. Marvin and George S. Deiwert

Ames Research Center

Moffett Field, Calif.

NATIONAL AERONAUTICS AND SPACE ADMINISTRATION • WASHINGTON, D. C. • JULY 1965

NASA TR R-224

CONVECTIVE HEAT TRANSFER IN PLANETARY GASES

By Joseph G. Marvin and George S. Deiwert

Ames Research Center
Moffett Field, Calif.

NATIONAL AERONAUTICS AND SPACE ADMINISTRATION

For sale by the Clearinghouse for Federal Scientific and Technical Information
Springfield, Virginia 22151 – Price $2.00

CONVECTIVE HEAT TRANSFER IN PLANETARY GASES

By Joseph G. Marvin and George S. Deiwert
Ames Research Center

SUMMARY

28674

Equilibrium convective heat transfer in several real gases was investigated. The gases considered were air, nitrogen, hydrogen, carbon dioxide, and argon. Solutions to the similar form of the boundary-layer equations were obtained for flight velocities to 30,000 ft/sec for a range of parameters sufficient to define the effects of pressure level, pressure gradient, boundary-layer-edge velocity, and wall temperature. Results are presented for stagnation-point heating and for the heating-rate distribution.

For the range of parameters investigated the wall heat transfer depended on the transport properties near the wall and precise evaluation of properties in the high-energy portions of the boundary layer was not needed. A correlation of the solutions to the boundary-layer equations was obtained which depended only on the low temperature properties of the gases. This result can be used to evaluate the heat transfer in gases other than those considered.

The largest stagnation-point heat transfer at a constant flight velocity was obtained for argon followed successively by carbon dioxide, air, nitrogen, and hydrogen. The blunt-body heating-rate distribution was found to depend mainly on the inviscid flow field.

For each gas, correlation equations of boundary-layer thermodynamic and transport properties as a function of enthalpy are given for a wide range of pressures to a maximum enthalpy of 18,000 Btu/lb.

INTRODUCTION

Convective heat transfer to bodies entering the earth's atmosphere has been studied extensively. No attempt will be made to reference all these investigations, but representative examples are references 1 to 3. Only a few investigators have examined the problem associated with flight into planetary atmospheres having constituent gases differing from air and these deal directly with stagnation-point heat transfer. (See, e.g., refs. 4 and 5.) Prior to these latter investigations, it was common to correlate heat-transfer results in terms of the transport and thermodynamic properties at the boundary-layer edge (i.e., see ref. 2), but as indicated in reference 5, a correlation for various dissociating gases was obtained in terms of molecular weight of the cold mixture. A correlation of this nature is much more convenient since estimates of heating in any number of gases seemed to be feasible without requiring the burdensome task of evaluating the transport properties at the boundary-layer edge. In light of these two apparently different modes of correlation, it seemed appropriate to study the relation of the transport properties to the heat transfer.

In a cursory look at this problem, pertinent thermodynamic and transport properties of several gases were compared because it is through these properties that differences in heat transfer would be expected to appear. This comparison illustrated some of the property differences between gases and these differences were investigated further to assess their effects on the convective heat transfer.

It is the purpose of this report to present the results of this investigation for several real gases, including air, and to point out the significant differences and similarities between the results for the various gases. The results were obtained by solving the boundary-layer equations for the gases, air, nitrogen, hydrogen, carbon dioxide, and argon, subject to the assumptions of local similarity and thermodynamic equilibrium. Solutions are presented for flight velocities to 30,000 ft/sec and for a range of parameters sufficient to define the influence of pressure, pressure gradient, wall temperature, and velocity at the edge of the boundary layer. The results are presented for stagnation-point heating and heating-rate distribution and are correlated in terms of the gas properties at low temperatures.

SYMBOLS

c_p	total specific heat
c_{p_i}	specific heat of species i
C_i	mass fraction of species i
D_{ij}	multicomponent diffusion coefficient
f	$\int_0^\eta \frac{u}{u_e}\,d\eta$
g	normalized total enthalpy, $\frac{H}{H_s}$
h	static enthalpy
H	total enthalpy $\left(h + \frac{u^2}{2}\right)$
H_s	stagnation enthalpy
k	total thermal conductivity
k_f	frozen thermal conductivity
m_i	molecular weight of species i
n	shape parameter, n = 1 for axisymmetric and n = 0 for two-dimensional
$\bar{n}$	total number of moles

p pressure

Pr total Prandtl number

q_w heat-transfer rate to the wall

q_y y component of the heat-flux vector

r body coordinate, shown in sketch, appendix A

T temperature

u velocity in direction of boundary-layer flow (i.e., velocity in x direction)

U_∞ free-stream velocity

v velocity normal to direction of boundary-layer flow (i.e., velocity in y direction)

x coordinate along wall

X_i mole fraction of species i

y coordinate normal to wall

β pressure-gradient parameter defined in equation (A21)

η transformed coordinate defined by equation (A12b)

μ viscosity

ξ transformed coordinate defined by equation (A12a)

ρ mass density

φ $\frac{\rho\mu}{\rho_w\mu_w}$

Subscripts

D value at onset of dissociation or ionization

e boundary-layer-edge value

o stagnation-point value

r reference value, see table I

w wall value

∞ free-stream value

PRESENTATION OF EQUATIONS

The problem considered is that of convective heat transfer in various gases. The equations necessary for describing this phenomenon are the conservation of mass, momentum, and energy equations. Along with these, relations describing the fluid state and transport properties are required. These equations are developed in appendix A and the resulting equations are presented below.

Heat-Flux Equation

The wall convective heat-flux equation for a chemically reacting mixture of gases in thermochemical equilibrium is

$$q_w = \frac{k_w}{c_{p_w}} \left(\frac{\partial h}{\partial y}\right)_w = \frac{\mu_w}{Pr_w} \left(\frac{\partial h}{\partial y}\right)_w \tag{1}$$

This equation can be solved when the transport properties and enthalpy gradient at the wall are known. For this study, the unknown in equation (1) is the enthalpy gradient which must be obtained by solving the boundary-layer equations.

Similar Boundary-Layer Equations

An appropriate set of equations for studying the effect of gas composition on the wall enthalpy gradient is the similar form of the boundary-layer equations. These particular equations are exact when similarity holds, such as in the stagnation region of a body, and they allow approximate prediction of the heating-rate distribution over bodies.

The similar boundary-layer equations in the familiar ξ and η coordinate system (see eq. (A12)) may be written in the following form:

$$(\varphi f'')' + ff'' + \beta \left(\frac{\rho_e}{\rho} - f'^2\right) = 0 \tag{2}$$

$$\left(\frac{\varphi}{Pr} g'\right)' + fg' + \frac{u_e^2}{H_s} \left[\left(\varphi - \frac{\varphi}{Pr}\right) f'f''\right]' = 0 \tag{3}$$

where

$$f' \equiv \frac{u}{u_e}, \qquad g \equiv \frac{H}{H_s}, \qquad \varphi \equiv \frac{\rho\mu}{\rho_w \mu_w}, \qquad \beta \equiv 2 \frac{d \ln u_e}{d \ln \xi}$$

and where the prime superscript represents differentiation with respect to η. The Prandtl number in equation (3) is the total Prandtl number obtained when the total specific heat and total thermal conductivity are used.

The boundary conditions on these equations are as follows:

$$f(o) = 0 \qquad f'(\infty) \rightarrow 1$$
$$f'(o) = 0$$
$$g(o) = g_w \qquad g(\infty) \rightarrow 1$$

The thermodynamic and transport property terms in these equations are treated as known functions of the static enthalpy. The pressure-gradient parameter β, wall temperature, pressure, and the term u_e^2/H_s are treated as parameters.

Equations for Heating Rate and Heating-Rate Distribution

Solutions to equations (2) and (3) are in the ξ and η coordinate system; therefore, with the aid of the transforming equations in appendix A, equation (1) is rewritten as

$$q_w = \frac{r^n \rho_w \mu_w u_e H_s}{Pr_w \sqrt{2\xi}} g'(o) \tag{4}$$

To obtain the heating-rate distribution over a body it is convenient to normalize equation (4) by the heating rate at a stagnation point given in reference 2 as

$$q_{w_o} = \frac{H_s}{Pr_w} \sqrt{2^n \rho_{w_o} \mu_{w_o} \left(\frac{du_e}{dx}\right)_o} \, g_o'(o) \tag{5}$$

Using equations (4) and (5) and assuming an isothermal surface, at a temperature small compared to the stagnation temperature, we may write the following heating-rate distribution equation

$$\frac{q_w}{q_{w_o}} = \frac{r^n \left(\frac{p_w}{p_{w_o}}\right)\left(\frac{u_e}{U_\infty}\right)}{\sqrt{2^{n+1} \int_o^x \left(\frac{p_w}{p_{w_o}}\right)\left(\frac{u_e}{U_\infty}\right) r^{2n} \, dx \left[\frac{d(u_e/U_\infty)}{dx}\right]_o}} \frac{g'(o)}{g_o'(o)} \tag{6}$$

THERMODYNAMIC AND TRANSPORT PROPERTIES

Solutions to the boundary-layer conservation equations depend on a knowledge of the thermodynamic and transport properties of the gas in question. The thermodynamic properties of pure gases can be calculated to good accuracy from spectroscopically determined constants. The situation concerning transport properties is more uncertain and their calculation depends on assumptions concerning the intermolecular potentials at the lower temperatures and on many uncertainties regarding collisions and diffusional phenomena at the higher temperatures. Despite these uncertainties, properties so calculated are probably representative of the actual values and, at least, should show how differences in gas composition affect heat transfer. This study was confined to the gases, air, nitrogen, hydrogen, carbon dioxide, and argon. The actual values of the properties for the various gases were compiled from information in references 6 to 15.

The properties were curve fitted as a function of enthalpy and used in the numerical solutions to the boundary-layer equations. This is explained in appendix B and the coefficients of each curve fit are tabulated in tables II through V.

To use these properties the gas considered must be in local thermochemical equilibrium and its atomic composition must correspond to that given by assuming its initial state was at standard conditions of pressure and temperature. Hence, using these properties in the boundary-layer equations implies equal diffusivity among the various species at all points in the boundary layer.

Before discussing the final results of the study, it is of interest to examine the variation of gas properties with enthalpy as these quantities enter the basic conservation equations as coefficients.

The gas-density ratios ρ_e/ρ are plotted against the enthalpy ratio h/H_s in figure 1. This figure is representative of the change in density with enthalpy at the stagnation region of a blunt body for a flight velocity of 30,000 ft/sec and a pressure of 0.1 atm. A significant difference in density between the various gases occurs at intermediate values of the enthalpy ratio. However, as stipulated in reference 1, differences of this magnitude probably have little influence on the wall enthalpy gradient obtained from the solution to the boundary-layer equations. Further investigation was undertaken to verify this point and the results are discussed later.

Figure 2 presents the variation of $\rho\mu/\rho_w\mu_w$ (hereafter defined as φ) with h/H_s for each gas. Air, nitrogen, carbon dioxide, and argon behave in a similar manner, showing some differences in level with particular values of h/H_s. Hydrogen exhibits the smallest variation of φ.

Figure 3 shows the changes in φ/Pr with h/H_s for each gas. This term reflects the changes in the ratio k/c_p superimposed on the density variation seen in figure 1. Fluctuation of the φ/Pr curves from $h/H_s = 1$ to $h/H_s = 0$ is related to the chemical reactions that take place during the

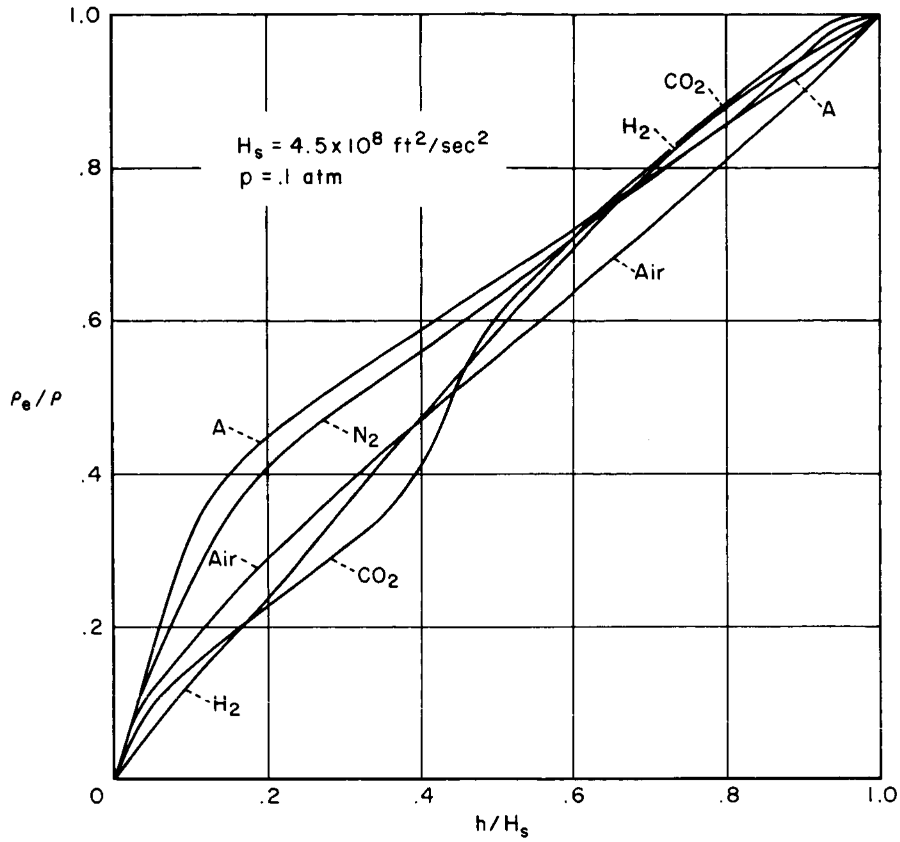

Figure 1.- Density variation with enthalpy for various gases.

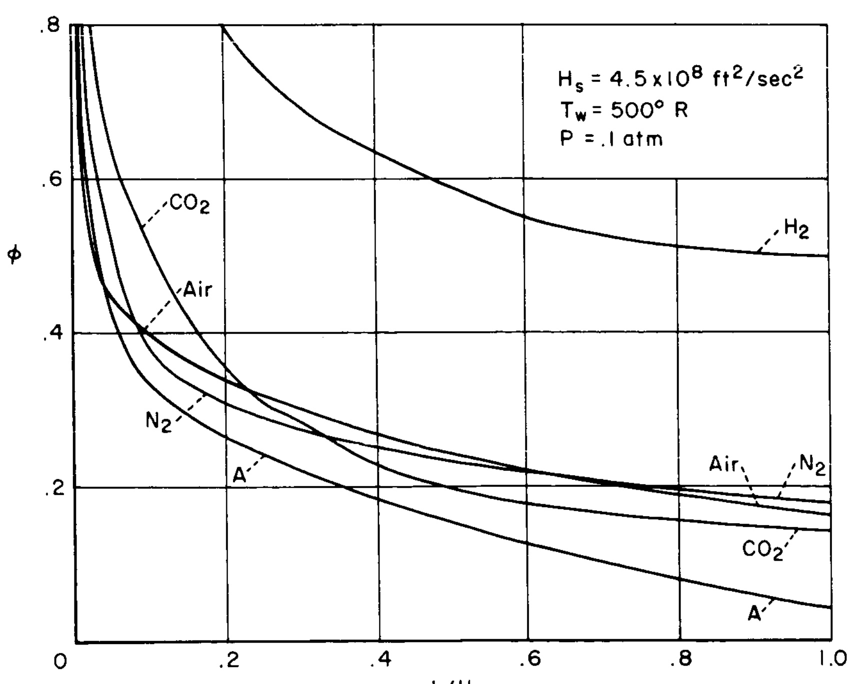

Figure 2.- Density-viscosity product variation with enthalpy for various gases.

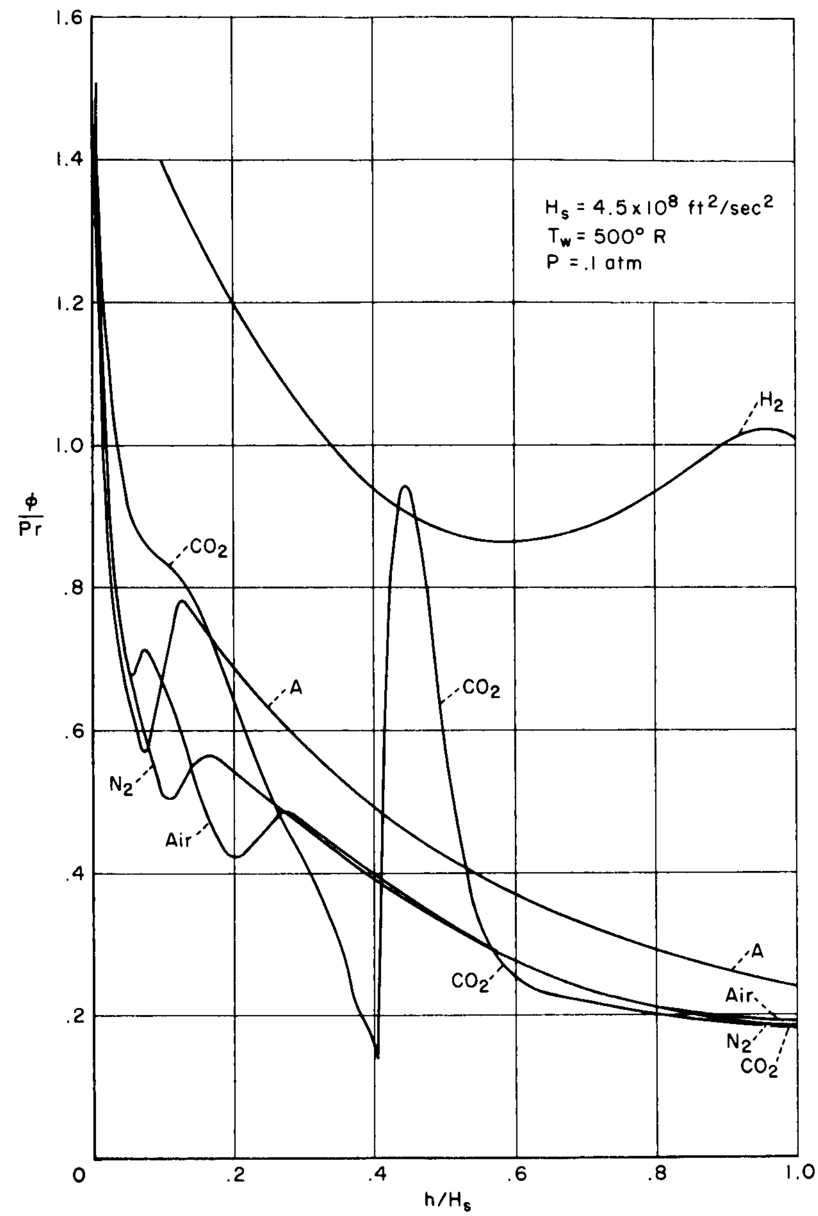

Figure 3.- Variation of φ/Pr with enthalpy for various gases.

recombination of various species through the boundary layer. These quantities depend both on the concentration gradients and concentrations of each species and therefore assume rather complicated behaviors. The fluctuations of φ/Pr are usually associated with the completion and onset of various reactions. For example, the species concentration of CO_2 taken from reference 12 and plotted in figure 4 shows that the first fluctuation occurs during the formation of the maximum amount of CO from free O and C and that the next notable fluctuation occurs during the final formation of CO_2 from the various dissociated species. The effect of this φ/Pr variation on the solution to the boundary-layer equations will be discussed later.

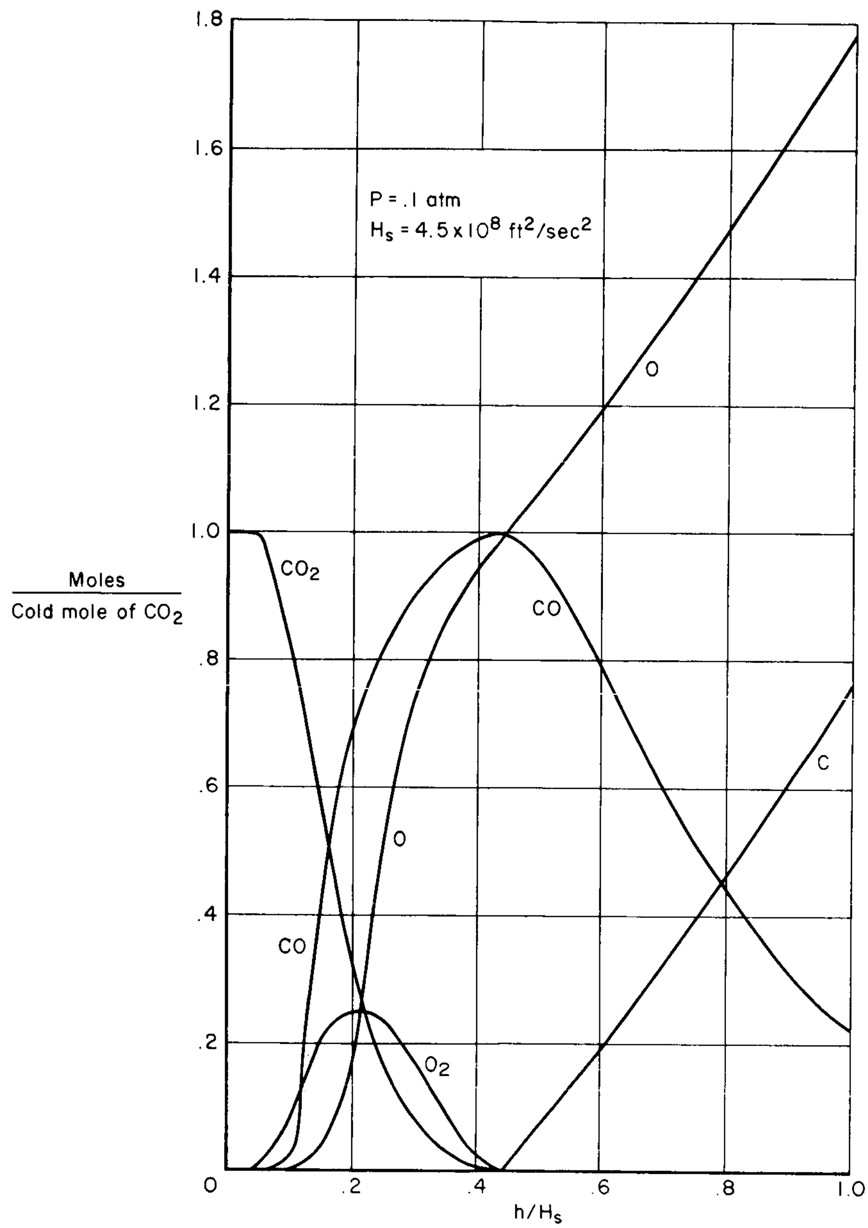

Figure 4.- Gas composition of CO_2 (mole per original cold mole of CO_2). Variation with static enthalpy (taken from ref. 12).

Pressure level can affect the property variations of each gas as illustrated in figure 5 where φ/Pr for N_2 and CO_2 for two pressures is shown. For N_2 there are only small differences in φ/Pr for the two pressures, whereas for CO_2 there is a marked difference. The other gases do not exhibit such wide differences with pressure level as CO_2, but the need to investigate the effect of pressure changes on the boundary-layer solutions for all the gases is evident.

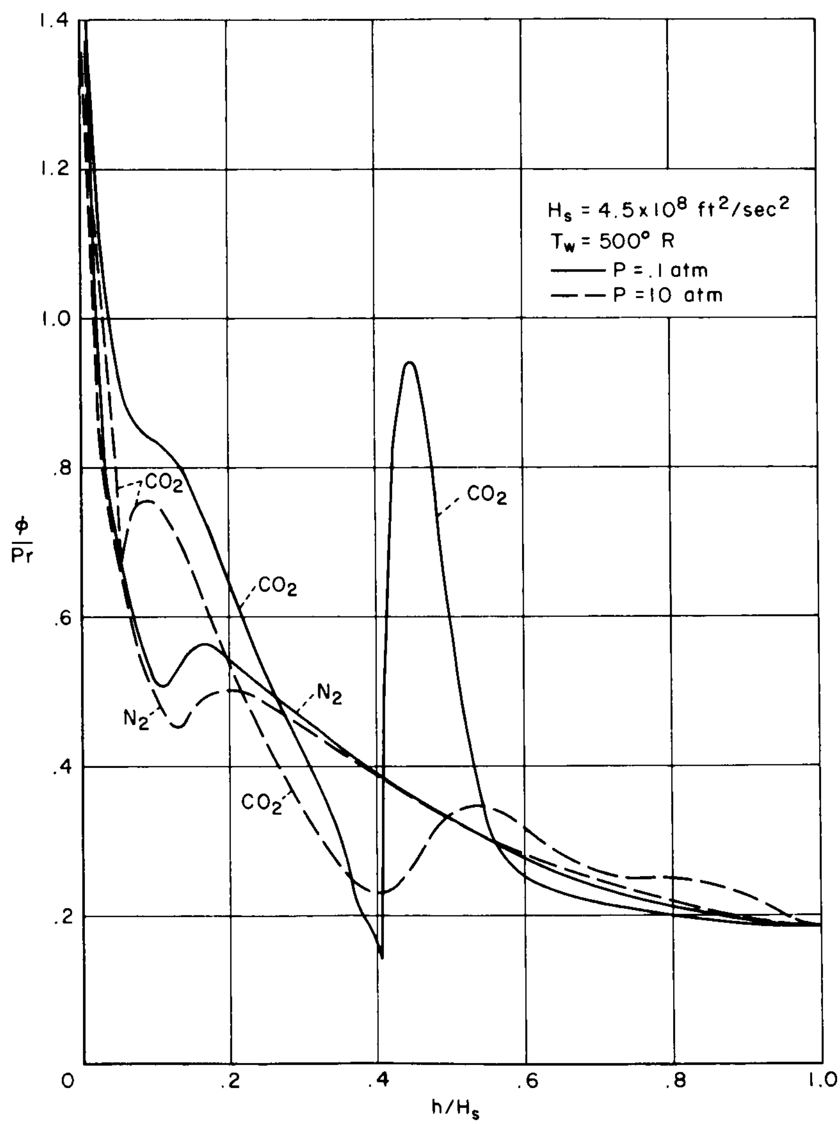

Figure 5.- Effect of pressure level on φ/Pr for N_2 and CO_2.

The comparisons made above are inconclusive insofar as telling how the differences in gas properties might affect solutions to the boundary-layer equations and, in particular, the wall enthalpy gradient. The next step is to solve the differential equations for various values of pressure, pressure gradient, boundary-layer-edge velocity, and wall temperature. The range for these was generally chosen as follows:

$$0 \leq \beta \leq 1$$

$$500^{\circ}\ R \leq T_w \leq 1850^{\circ}\ R$$

$$0 \leq \frac{u_e^2}{H_s} \leq 1$$

$$10^{-3} \leq p_e \leq 10 \text{ atm}$$

RESULTS AND DISCUSSION

Similar Solutions

Solutions to the boundary-layer equations for each of the gases when certain external flow parameters and wall conditions were varied are summarized next. Generally, each gas behaved in the same way; for example, the heat-transfer parameter $g'(o)/1-g_w$ increased with increasing wall temperature and increasing pressure-gradient parameter β; it decreased with increasing flight velocity or total enthalpy; for practical purposes it was unaffected by changes in the dissipation parameter u_e^2/H_s and the pressure level.

A correlation which included all the input parameters was needed to illustrate the important results of the solutions. Such a correlation was presented by Fay and Riddell (ref. 2) and subsequently by Kemp, Rose, and Detra (ref. 3). These investigators found that for dissociated air (for flight velocities to 30,000 ft/sec) the heat-transfer parameter $g'(o)/1-g_w$ correlated with φ_e. This term reflects implicitly the changes in flight velocity and wall temperature; that is, at constant wall temperature it decreases with increasing flight velocity; at constant flight velocity it increases with increasing wall enthalpy or temperature. In addition φ_e appeared to account for the over-all changes in thermodynamic and transport properties through the boundary layer, implying that subsequent differences in the numerical values of the transport properties would not affect the correlation equation. The investigators of reference 3 found that the pressure-gradient parameter was accounted for by assuming that the enthalpy gradient varied as $(1 + \text{constant} \sqrt{\beta})$ and also that the dissipation term $(u_e^2/H_s)[(\varphi - \varphi/Pr)f'f'']'$ affected the solutions to a minor degree. This correlation was attempted for each of the gases considered herein.

The results are presented in figures 6 through 10. In these figures the heat-transfer parameter $g'(o)/1-g_w$ is divided by Pr_w and by a term which accounted for the pressure-gradient parameter (i.e., $(1 + \text{constant}\sqrt{\beta})$). The various symbols represent different values of the pressure-gradient parameter.

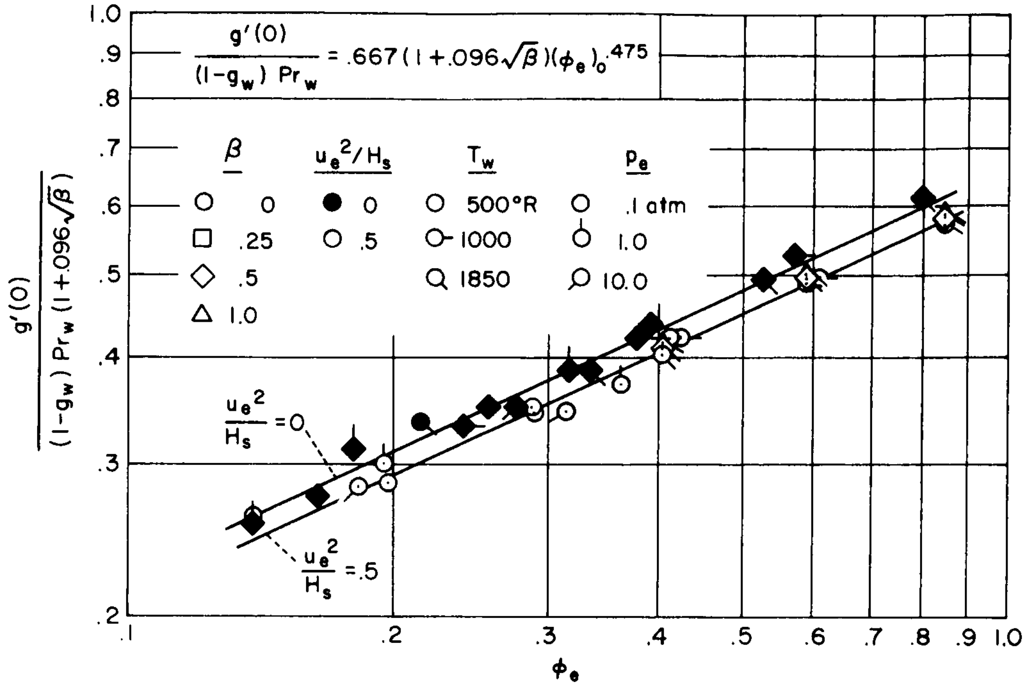

Figure 6.- Heat-transfer parameter correlation for air.

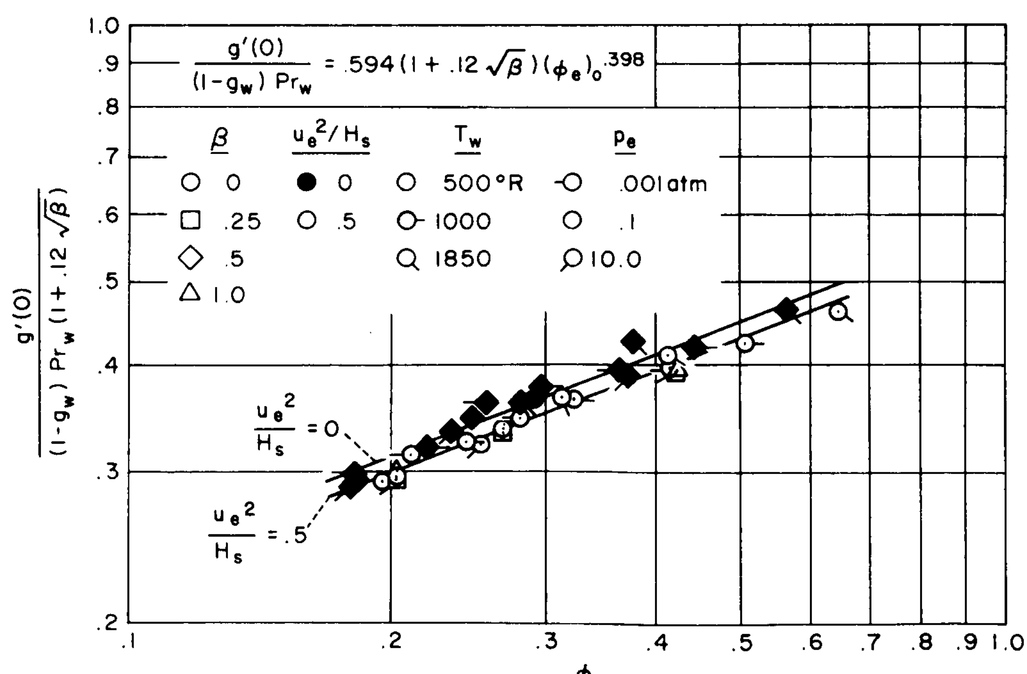

Figure 7.- Heat-transfer parameter correlation for nitrogen.

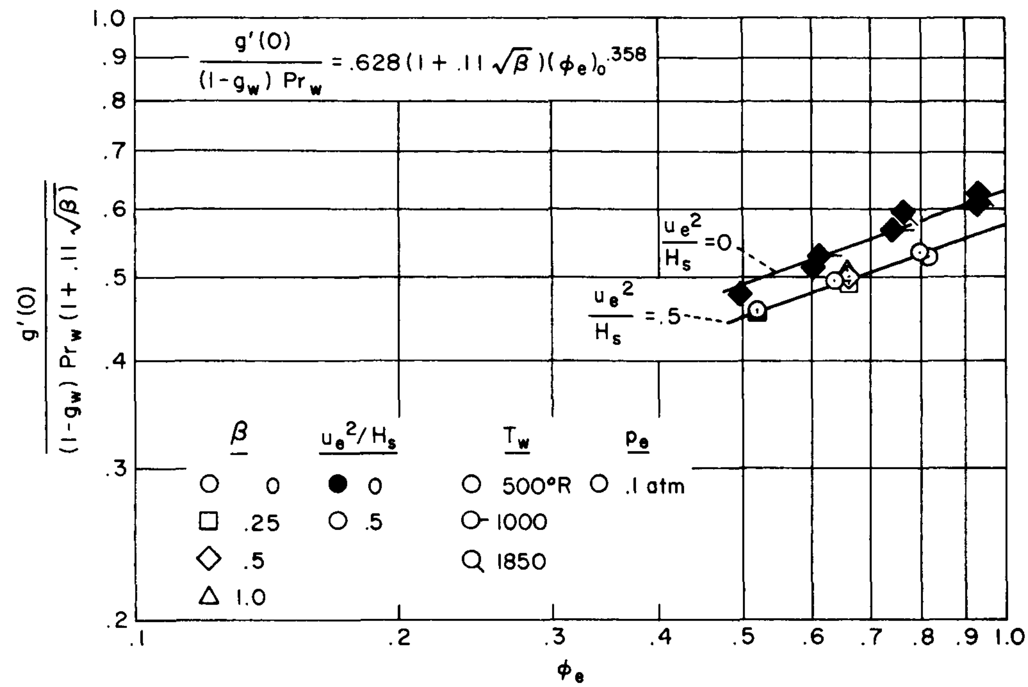

Figure 8.- Heat-transfer parameter correlation for hydrogen.

Symbols are flagged to represent solutions for different wall temperatures and different pressures. Symbols are filled to represent solutions for different values of u_e^2/H_s. For the investigated range of parameters the solutions correlate about straight lines of the same slope fitted to the solutions for constant values of u_e^2/H_s. The two straight lines shown on each figure represent curve fits through the solutions for $u_e^2/H_s = 0$ and $u_e^2/H_s = 0.5$.

The first important aspect of the correlation is the relatively small dependence of the heat-transfer parameter on β. The term $(1 + \text{constant}\sqrt{\beta})$ found in the ordinate of each figure is never much larger than 1.0 because the value of the constant, although slightly different for each gas, is numerically small.

The correlation figures point out that the dissipation term also has a relatively small effect on the enthalpy gradient. This is clearly demonstrated in figure 9 where the results for CO_2 are plotted. At three distinct locations along the correlating line for $u_e^2/H_s = 0$ the dissipation parameter was varied between 0 and 1 for a constant pressure and wall temperature and a solid line (practically horizontal) joins these solutions. For each successive change in u_e^2/H_s the value of φ_e increases because the static enthalpy decreases at the boundary-layer edge while the enthalpy gradient changes a small amount. The largest changes in the enthalpy gradient occur at the largest values of φ_e, but for practical purposes these are negligible. Each of the gases showed a similar dependence on the dissipation parameter. This allows a convenient equation for the enthalpy gradient to be expressed in terms of the stagnation value of φ_e and β. These equations are presented in each of the figures. The advantage of these equations is that the enthalpy gradient ratio in the heating-rate distribution (see eq. (6)) can be determined without computing the local value of the density-viscosity product.

Next, these correlations demonstrate the effect of changes in wall temperature and pressure. As the wall temperature increases, φ_e increases. At the same time, the heat-transfer parameter increases so that a straight line joins solutions for identical values of u_e^2/H_s. Note that differences in Pr_w, resulting from changes in wall temperature, did not introduce scatter into the correlations. Likewise, changes in pressure cause changes in φ_e with corresponding changes in the heat-transfer parameter such that the correlation line is maintained. The scatter of the results about the correlating line due to pressure and temperature changes is small for practical applications. These changes introduce more scatter for CO_2 (fig. 9) than for air, hydrogen, and nitrogen. An estimate of the magnitude of this scatter is obtained by comparing some of the results for $u_e^2/H_s = 0$ with the straight-line curve fit to these points. It can be seen that changes in pressure level introduce more scatter than wall temperature.

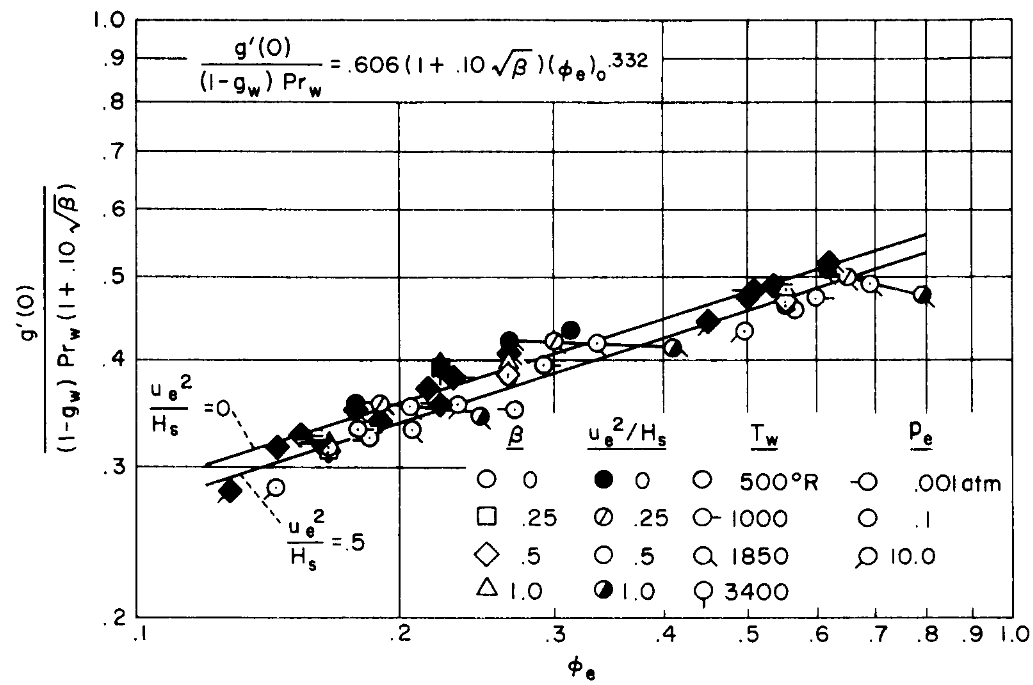

Figure 9.- Heat-transfer parameter correlation for carbon dioxide.

Argon (fig. 10) did not correlate as well as the other gases. For this gas, only the solutions for the lowest value of the wall temperature were used for obtaining the straight-line fits. At each velocity (constant $\rho_e\mu_e$) increasing the wall temperature increases both the enthalpy gradient and φ_e. However, decreasing φ_e by maintaining a constant wall temperature and increasing the flight velocity does not cause a corresponding decrease in the enthalpy gradient. This is in direct contrast to the solutions obtained for the other gases. As a result, the slope of the correlating line is much smaller than for the other gases. Pressure also affects the solutions for argon more than other gases; for example, at 20,000 ft/sec, results for 10^{-3} and 10^{-1} atm agree very well but differ from that for 10 atm by about 10 percent, although this is not considered significant for practical applications.

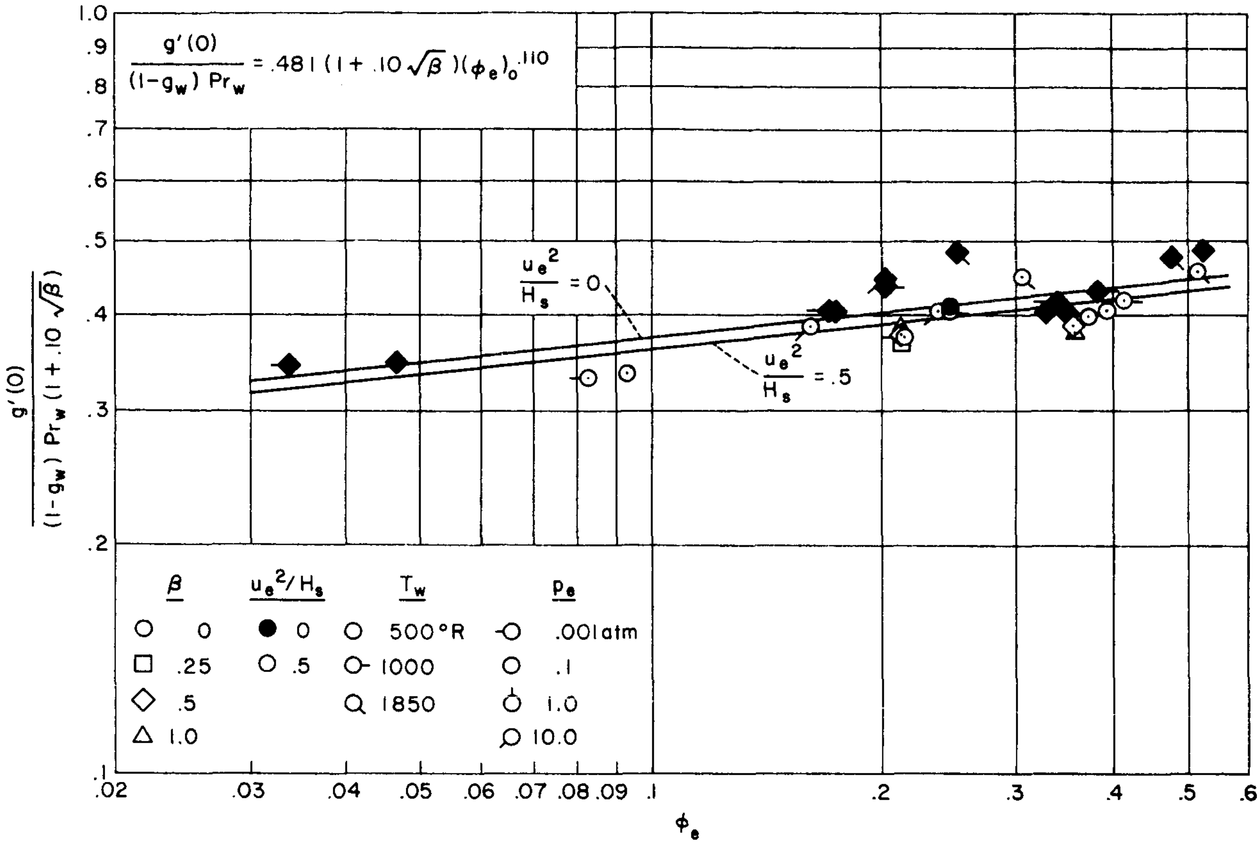

Figure 10.- Heat-transfer parameter correlation for argon.

The behavior of argon is quite similar to that of air when the total enthalpy reaches the value where ionization significantly affects the viscosity used in evaluating φ_e (see, e.g., ref. 16).

Correlations in terms of φ_e are not without shortcomings. First, the correlation equations can be used only over the range of φ_e for which they are developed. This is substantiated in the results for air given in references 16 and 17 and will be demonstrated later in this study. Secondly, a single correlation equation in terms of φ_e is not obtained for all the gases and therefore the results are not general enough for computing the heat transfer in gases other than those being considered. Finally, the correlation lacks the quality of accounting for the constancy of the enthalpy gradient with varying u_e^2/H_s. Two unsuccessful attempts were made to eliminate these shortcomings. The integrals of φ and φ/Pr across the boundary layer were investigated as single correlating factors for all gases. However, they resulted in individual correlations for each gas which were no better than those for which φ_e alone was used. Hence, a detailed study of the effect of the property variations on the solutions was undertaken. The results are presented next and are then used to obtain a single correlation which is useful for estimating heating rates in various gases.

Effect of Gas Properties on Similar Solutions

Some of the solutions in carbon dioxide gas are considered first since they are representative of the results for other gases. Variations of velocity f', enthalpy g, and the property terms across the boundary layer are given in figures 11, 12, and 13 for a pressure-gradient parameter of 1/2 and for three flight velocities. Two values of the dissipation parameter were used, one representing a stagnation point and the second, a point on the vehicle where the local boundary-layer outer-edge velocity is $\sqrt{H_s/2}$. The local boundary-layer-edge velocity influences the solutions in two ways: first, it changes the static enthalpy distribution across the boundary layer which in

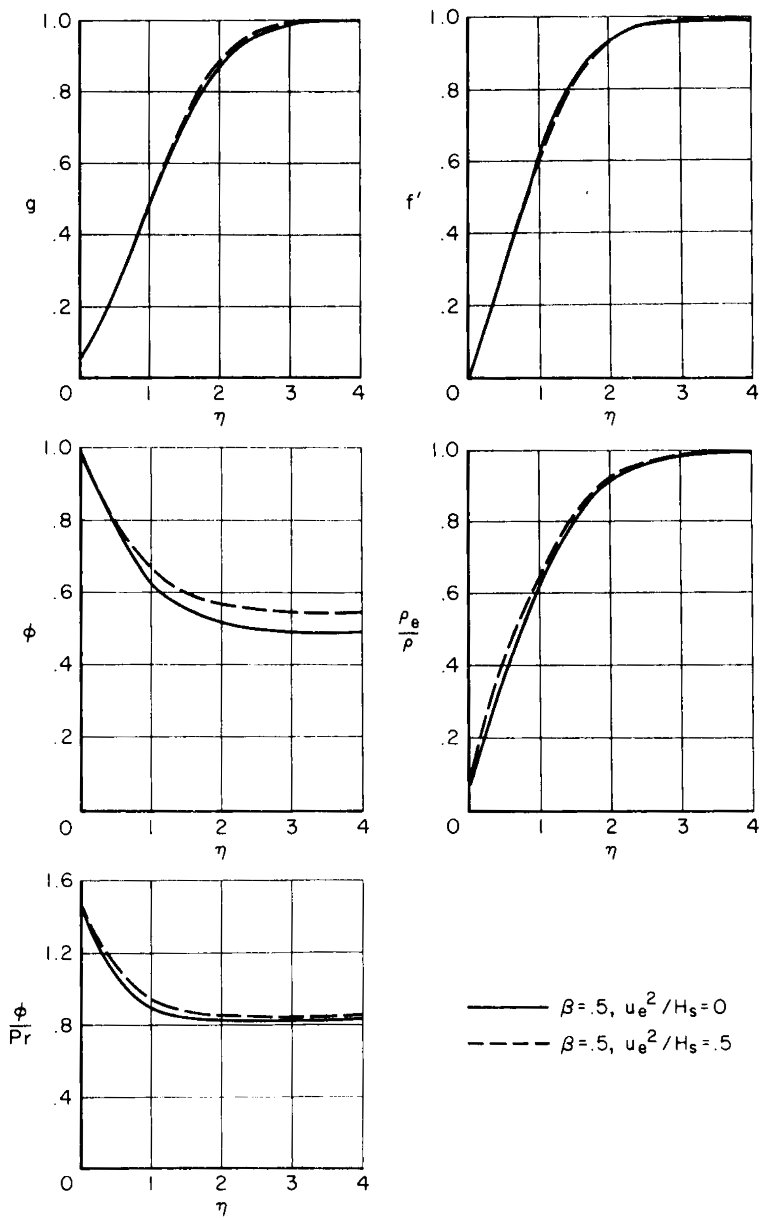

Figure 11.- Comparison of boundary-layer profiles; CO_2, U_∞ = 10,000 ft/sec, T_w = 500° R, and p = 0.1 atm.

turn changes the fluid property variations; secondly, it introduces the dissipation term in the energy equation (see eq. (3)). It will be shown subsequently that the latter effect is very small and therefore the comparison of the pairs of solutions in figures 11 through 13 shows the effects of varying property distributions through the boundary layer.

In figure 11, the enthalpy, velocity, and property terms vary smoothly between their wall and boundary-layer-edge values. The relatively small change in property profiles, brought about by including u_e^2/H_s, does not affect the enthalpy gradient at the wall to any significant extent. In figure 12 where the total enthalpy has been increased, significantly different

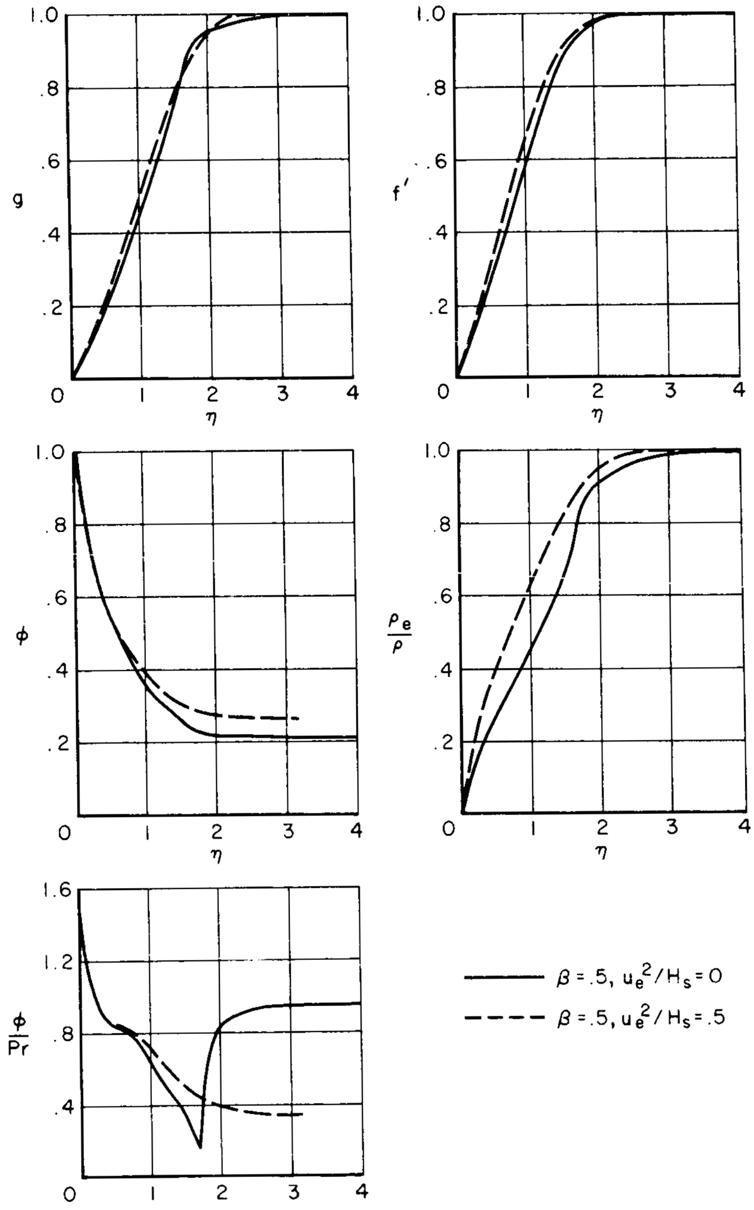

Figure 12.- Comparison of boundary-layer profiles; CO_2, U_∞ = 20,000 ft/sec, T_w = 500° R, and p = 0.1 atm.

property variations are obtained, and yet the enthalpy profiles, especially near the wall, do not reflect these differences. This is especially true for the enthalpy gradients at the wall which differ for this case by less than 10 percent. Similar conclusions are reached from figure 13. The results indicate that property variations "far away" from the wall (especially for φ/Pr) have a rather small effect on the enthalpy gradient at the wall and therefore on the heat transfer. Another interesting aspect of the comparison which will be used later is the behavior with total enthalpy (or flight velocity) of the φ and φ/Pr terms near the wall. The absolute value of the slope of these terms near the wall increases with flight velocity while the wall enthalpy gradient decreases (recall the results for varying free-stream velocity in figs. 6 to 10).

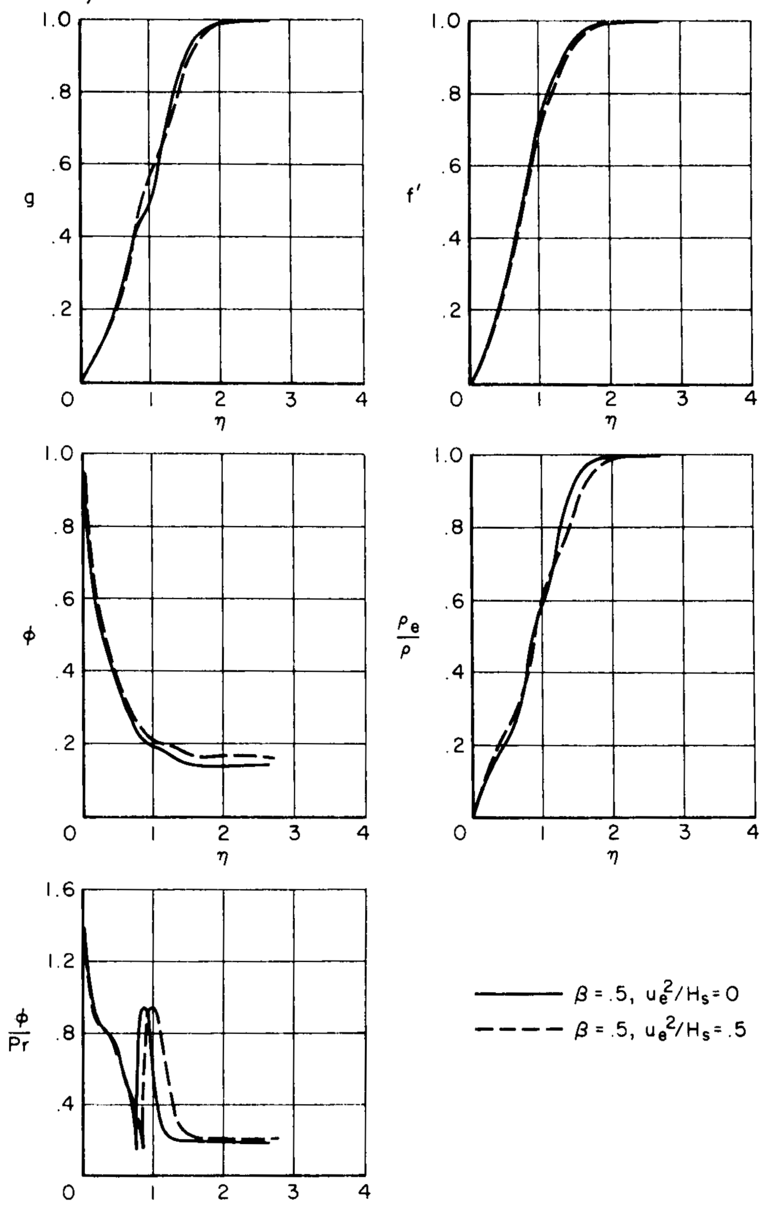

Figure 13.- Comparison of boundary-layer profiles; CO_2, U_∞ = 30,000 ft/sec, T_w = 500° R, and p = 0.1 atm.

It was mentioned above that the effect of including the dissipation term in the energy equation became evident only through its effect on the fluid property variation through the boundary layer. To show this, the magnitude of various terms in the energy equation (see eq. (A26)) for the flight velocity of 20,000 ft/sec is compared in figure 14 with those obtained when the

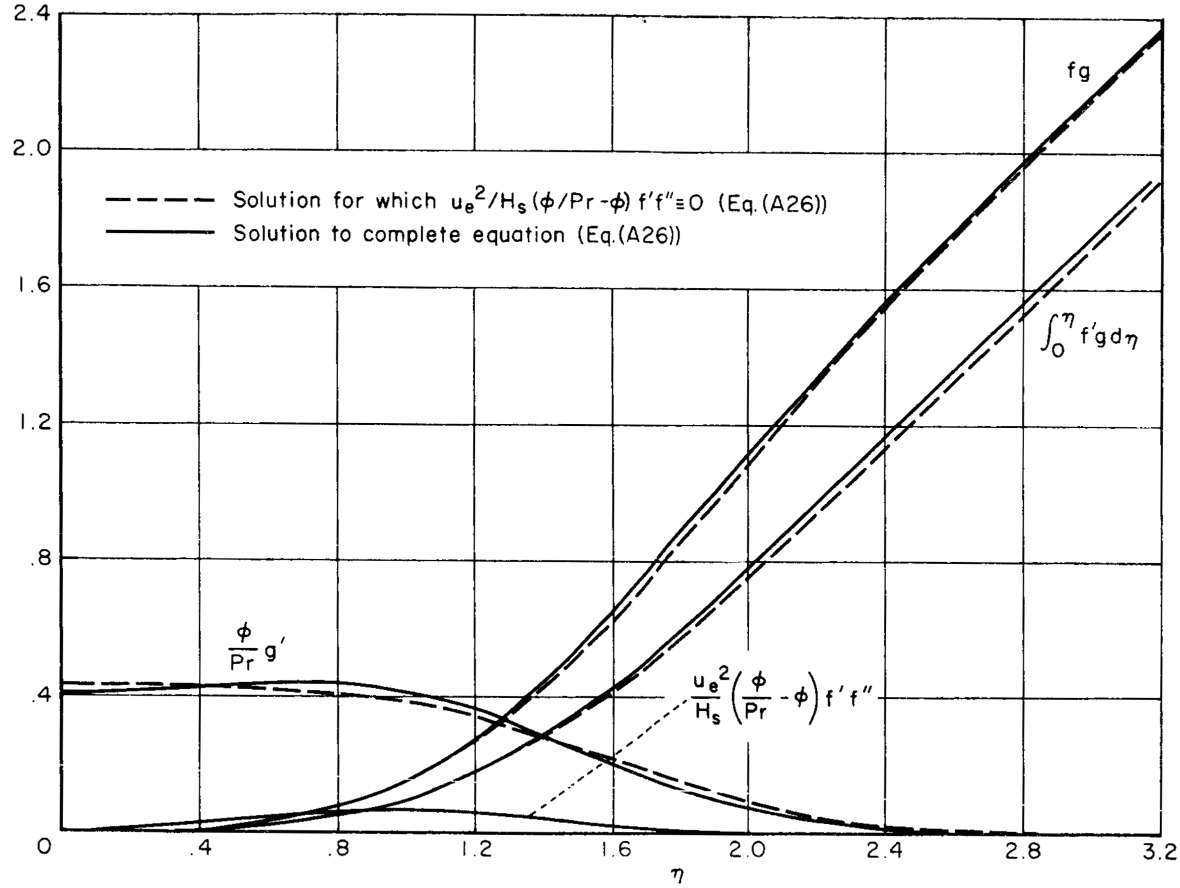

Figure 14.- Magnitude of terms occurring in energy equation; CO_2, U_∞ = 20,000 ft/sec, T_w = 500° R, and p = 0.1 atm.

dissipation term was zero. The value of U_e^2/H_s was one-half in both cases. This figure shows that the dissipation term itself $(u_e^2/H_s)[(\varphi - \varphi/Pr)f'f'']'$ has little influence on the solution and especially on the wall enthalpy gradient. Spot-check solutions for other velocities and for other gases gave the same result.

It is also appropriate at this point to indicate how the density term ρ_e/ρ affects the determination of the enthalpy gradient. Several solutions to the boundary-layer equations for different density distributions showed that the solutions were insensitive to arbitrary variations of ρ_e/ρ. For example, using the ρ_e/ρ distribution for CO_2 and the φ and φ/Pr distribution for N_2 to obtain a stagnation-point solution at 30,000 ft/sec resulted in a negligible change in enthalpy gradient from the corresponding nitrogen solution.

Thus far, it has been shown that the variation of the terms φ and φ/Pr "close" to the wall rather than that "far" from the wall affects the enthalpy gradient and that the rate of change of these property terms with η near the wall influences this gradient. For this reason a single correlation curve with φ_e is not obtained for all gases. This is illustrated in figure 15 where the stagnation-point profiles for some of the gases are plotted for a flight velocity of 30,000 ft/sec, a pressure of 0.1 atm, and a wall temperature of 500° R. Also included are the computed values for $g'(o)/1-g_w$. Observe that the values of φ_e for the gases differ but that the enthalpy gradients do not, provided the variations of the property terms near the wall are similar (i.e., compare the enthalpy gradients and the property profiles "near" the wall for CO_2, N_2, and A). These results suggest that any general correlation should probably be based on properties evaluated "near" the wall.

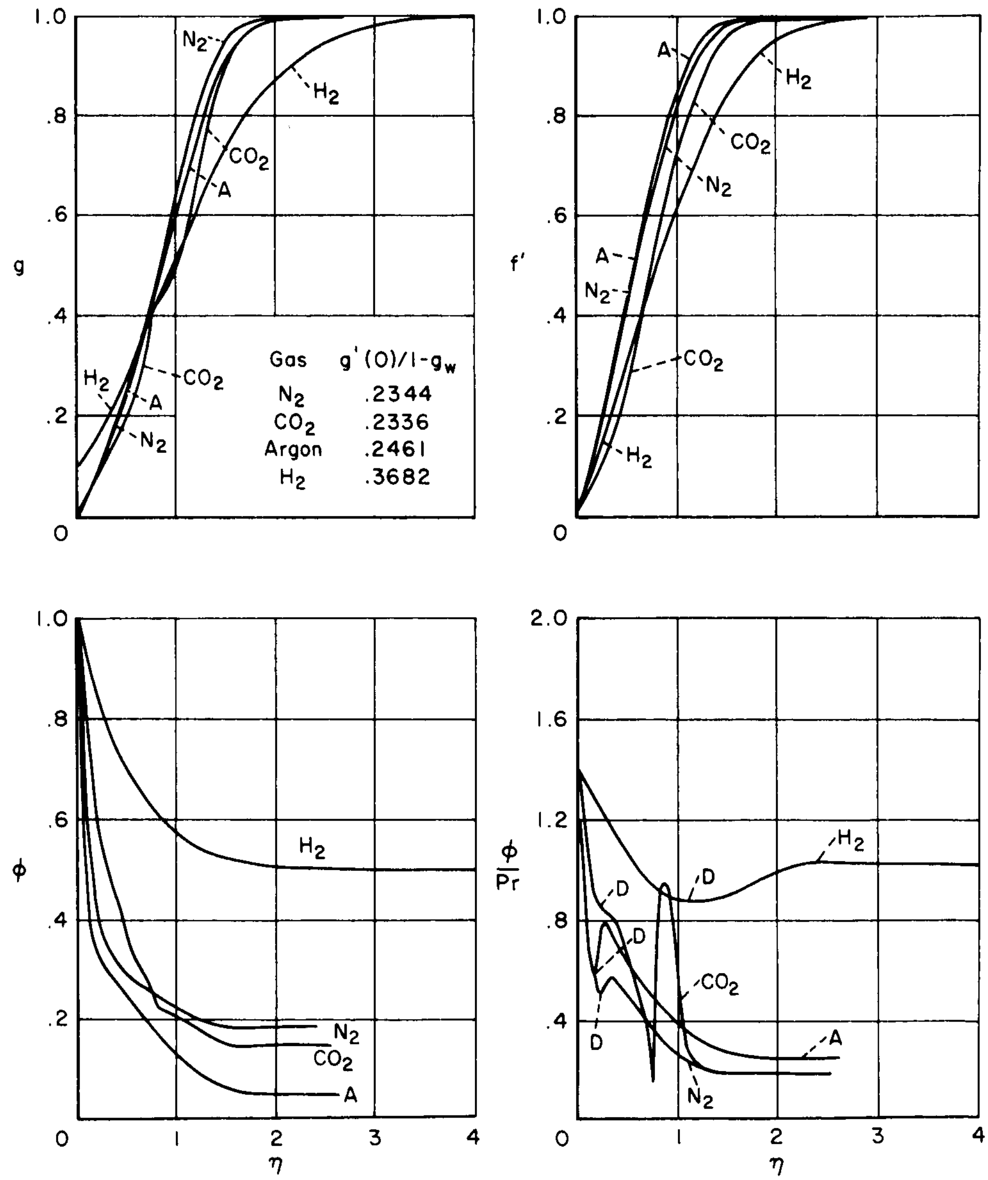

Gas	$g'(0)/1-g_w$
N_2	.2344
CO_2	.2336
Argon	.2461
H_2	.3682

Figure 15.- Boundary-layer profiles for various gases at a stagnation point; U_∞ = 30,000 ft/sec, p = 0.1 atm, and T_w = 500° R.

The insensitiveness of the solutions to the variation of the transport properties in the higher energy portions of the boundary layer indicates that precise evaluation of the transport properties at the higher enthalpies may not be critical for determining the equilibrium convective heat transfer. Calculations were made to determine how much the properties could be changed before significant differences in the enthalpy gradients appeared. Typical results are presented in figure 16 where the profiles for a stagnation point in carbon dioxide are plotted. First, the true φ/Pr variation was changed by fixing the Prandtl number constant (at its wall value) across the boundary layer. The velocity and enthalpy profiles in the lower energy portion of the

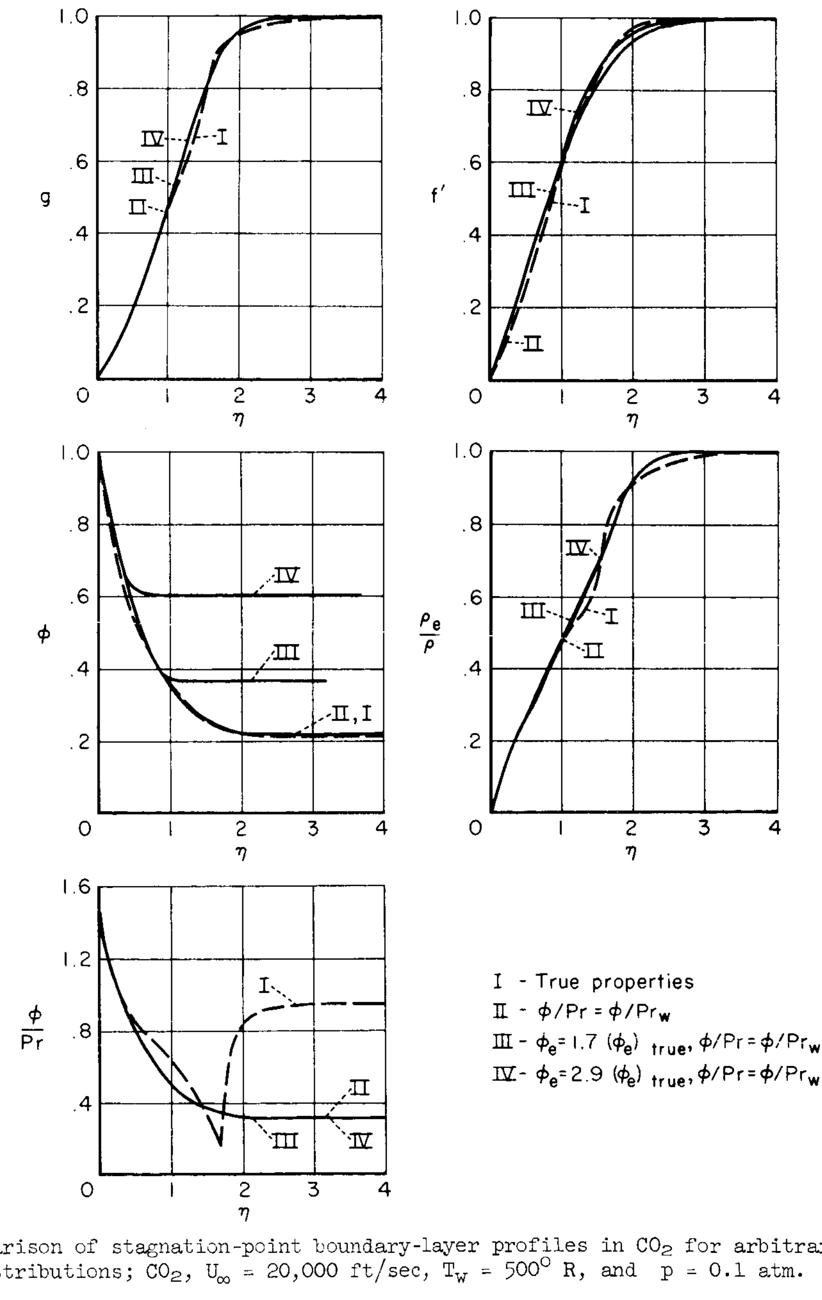

Figure 16.- Comparison of stagnation-point boundary-layer profiles in CO_2 for arbitrary φ and φ/Pr distributions; CO_2, U_∞ = 20,000 ft/sec, T_w = 500° R, and p = 0.1 atm.

boundary layer are not changed and the enthalpy gradients differed by less than 5 percent. Next, solutions for several different φ profiles were obtained by arbitrarily fixing φ at a constant value at some point in the boundary layer; the enthalpy and velocity profiles and the enthalpy gradient did not change significantly. (For these cases the φ/Pr variation with constant Prandtl number described above was used.) Calculations for various velocities demonstrated that large differences in μ_e or $(k/c_p)_e$ do not significantly affect the value of the enthalpy gradient. One additional case was computed that is worthy of comment. For a stagnation-point solution at 30,000 ft/sec, φ/Pr (where $Pr = Pr_w$) was allowed to vary normally until η reached a value of 1; from there φ/Pr was increased until at the boundary-layer edge it was 25 times its normal value. The enthalpy gradient was increased only 50 percent over the correct value. Concurrent with the present investigation, reference 18 determined the effect of uncertainties in the thermal conductivity of air on the stagnation-point heat transfer. Their conclusions are in substantial agreement with those made above. These results vividly illustrate that correlation equations in terms of boundary-layer outer-edge properties should be used only over the range of φ_e for which they are derived.

Correlation of the Heat-Transfer Parameter in Terms of Low Temperature Properties

The results described above were used as a basis for obtaining a single correlation of the wall enthalpy gradients for all the gases. It seemed reasonable that the wall gradient would correlate on an "average" derivative of the "near-wall" property terms, and during the course of making arbitrary changes in the property variations it was determined that changes beyond the point where the φ/Pr variation reached a minimum or inflection did not seriously alter the enthalpy gradient at the wall. The correlation was obtained by using the absolute value of the average slope of φ with h/H_s, that is,

$$\left|\frac{\overline{d\varphi}}{d(h/H_s)}\right| = \left|\frac{\int_{h_w/H_s}^{h_D/H_s}\left[\frac{d\varphi}{d(h/H_s)}\right]d\left(\frac{h}{H_s}\right)}{\frac{h_D}{H_s} - \frac{h_w}{H_s}}\right| = \left(\frac{1 - \varphi_D}{\frac{h_D}{H_s} - \frac{h_w}{H_s}}\right)$$

Both h_D and φ_D were evaluated at the point in the boundary layer where dissociation (or ionization for argon) was just beginning. In particular, this point was chosen so that for the dissociating gases Z (the ratio of molecular weights) was 1.01 and for argon α (the degree of ionization) was 0.001. The points in the boundary layer where these conditions prevailed were associated with the points where φ/Pr obtained its first minimum or inflection (e.g., see φ/Pr in fig. 15). At the enthalpy h_D, only small amounts of dissociated or ionized species are present in the gases, but the concentrations and concentration gradients of the various species are sufficient to cause the ratio k/c_p to remain constant or decrease as reflected by the φ/Pr term. Figure 17 shows the correlation of $[g'(o)/1-g_w]\sqrt{\rho_w\mu_w/(\rho\mu)_{T=500^\circ R}}$. The stagnation-point solutions of the present investigation are included (with the

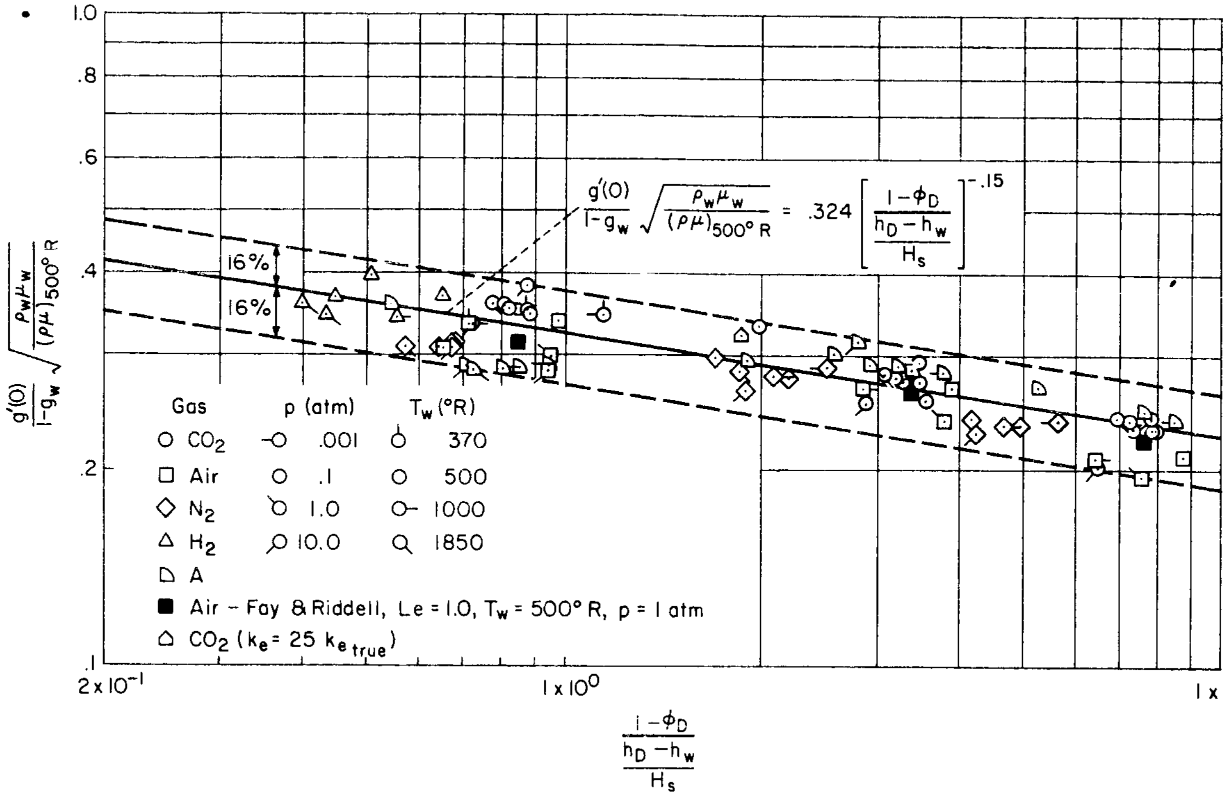

Figure 17.- Correlation of stagnation-point solutions for all gases.

exception of some hydrogen cases for which no dissociation occurred) and are found to correlate within ±16 percent. The term $\sqrt{\rho_w\mu_w/(\rho\mu)_{T=500^\circ R}}$ was included to reduce some scatter due to wall temperature variations. Also correlated are several solutions of reference 2 (Lewis number equal to 1.0) with values of h_D and φ_D given in reference 6 corresponding to a pressure of 0.1 atm and Z (ratio of molecular weights) of 1.01. The solution described earlier where $(k/c_p)_e$ was 25 times the true value is also included. For this case h_D and φ_D were evaluated at the point in the boundary layer where φ/Pr reached a minimum. The equation describing the correlation is

$$\frac{g'(o)}{1 - g_w}\sqrt{\frac{\rho_w\mu_w}{(\rho\mu)_{T=500^\circ R}}} = 0.324\left[\frac{1 - \varphi_D}{(h_D/H_s) - (h_w/H_s)}\right]^{-0.15} \tag{7}$$

If the enthalpy gradients for other values of β and $u_e{}^2/H_s$ are desired, they can be obtained by multiplying the corresponding stagnation-point gradient by the factor $0.93\,(1 + 0.10\sqrt{\beta})$. This factor uses an average value of the constants in the expression $(1 + \text{constant}\sqrt{\beta})$ in figures 6 to 10.

Other choices for determining the slope of the "near-wall" properties were also investigated. The best results were obtained by using a weighted average slope of φ/Pr with h/H_s over the same limits of integration used above. This resulted in a correlation of the stagnation-point solutions to within ±13 percent. This is about the smallest percentile range that can be obtained using property derivatives with respect to h/H_s as a correlation parameter. The equation describing this result is

$$\frac{g'(o)}{1 - g_w}\sqrt{\frac{\rho_w\mu_w}{(\rho\mu)_{T=500^\circ\,R}}} = 0.37\left[\frac{(\varphi/Pr)_w^2 - (\varphi/Pr)_D^2}{\int_{h_w/H_s}^{h_D/H_s}(\varphi/Pr)\,d(h/H_s)}\right]^{-0.12} \tag{8}$$

Obviously, the simplicity in applying equation (7) outweighs the small correlation improvement given by equation (8).

The correlation in terms of the property derivatives does not contain the shortcomings inherent in the correlations in terms of φ_e. First, a single correlation equation arises which can be used to predict the enthalpy gradient in gases other than those being considered. In application, this becomes a rather simple task since the correlation depends on relatively low temperature properties which are calculable for pure gases or gas mixtures by the methods described in reference 19. The correlation can be extrapolated into a range of enthalpy where both dissociation and ionization occur together in the boundary layer, as will be shown subsequently by demonstrating reasonably good agreement between heating rates calculated from the present correlation equation and those predicted by theories accounting for the effects of ionization on the transport properties and with actual shock-tube data. Finally, the correlation accounts for the constancy of the enthalpy gradient with u_e^2/H_s.

Stagnation-Point Heat Transfer

The heat-transfer parameter, $g'(o)/1-g_w$, was used to describe the results of the similar solutions to the boundary-layer equations. The next concern is how these results apply to the determination of the heat transfer to a body.

First, it is informative to develop specific equations for stagnation-point heat transfer in each gas so that the relative levels of heating rate for comparable conditions of flight velocity and stagnation-point pressure can be observed.

If a Newtonian pressure distribution in the vicinity of the stagnation region is assumed, the equation for the velocity gradient in equation (5) becomes

$$\left(\frac{du_e}{dx}\right)_o = \frac{1}{R}\sqrt{2\left(\frac{p_o - p_\infty}{\rho_{e_o}}\right)} \tag{9}$$

For simplicity p_∞ is neglected in what follows. Substituting equation (9) into equation (5) and multiplying both sides of the resulting equation by $\sqrt{R/p_o}$ gives

$$q_o\sqrt{\frac{R}{p_o}} = \frac{H_s}{Pr_w}\sqrt[4]{\frac{8(\rho_w\mu_w)^2}{p_o\rho_{e_o}}}\,g'(o) \tag{10}$$

The right side of equation (10) was computed for each gas for a range of stagnation pressures from 10^{-3} to 10 atm, wall temperatures from 500° to 1,850° R, and total enthalpies corresponding to flight velocities from 10,000 to 30,000 ft/sec. In this determination the value of $g'(o)$ from the boundary-layer solutions was used and not the correlations described above. The results were correlated within 10 percent by an equation of the form

$$\frac{q_o\sqrt{R/p_o}}{1 - g_w} = \bar{C}(\bar{U}_\infty)^N \tag{11}$$

where $\bar{U}_\infty$ is dimensionless and equals U_∞ divided by 10,000 ft/sec. In most cases the deviation of the computed value from that given by equation (11) was much smaller than 10 percent. Equation (11) is plotted in figure 18 and the constants $\bar{C}$ and N are tabulated. For a given flight velocity, argon has the highest stagnation-point heat transfer followed successively by CO_2, air, N_2, and H_2. For a given flight velocity, the stagnation-point heating in CO_2, air, and nitrogen is nearly the same. For hydrogen, the heating rate is not very large compared to the other gases over the range of velocity considered.

Although equations of the form given by equation (11) are very useful, their extension to higher velocities and to other gases is not straightforward since the constants $\bar{C}$ and N are valid only in the range of velocity considered here and are not readily expressed as functions of gas properties. Therefore it becomes necessary to develop a more general equation. Substituting equation (7) into equation (5) results in the following heating-rate equation for an axisymmetric body

$$q_o = \frac{0.324}{Pr_w}\sqrt{2(\rho\mu)_{T=500^\circ\,R}\left(\frac{du_e}{dx}\right)_o}\left[\frac{1 - \varphi_D}{(h_D/H_s) - (h_w/H_s)}\right]^{-0.15} H_s(1 - g_w) \tag{12}$$

Furthermore, using equation (9) and the approximation, $H_s \approx U_\infty^2/2$, we can rewrite equation (12) as

$$\frac{q_o\sqrt{R/p_o}}{1 - g_w} = \frac{0.360}{Pr_w}\sqrt[4]{\frac{1}{2}\,\frac{\left[(\rho\mu)_{T=500^\circ\,R}\right]^2}{p_o\rho_{e_o}}}\left(\frac{1 - \varphi_D}{h_D - h_w}\right)^{-0.15} U_\infty^{1.7} \tag{13}$$

To obtain equation (13) in the units, Btu/ft^2-sec (ft/atm)$^{1/2}$, it is rewritten

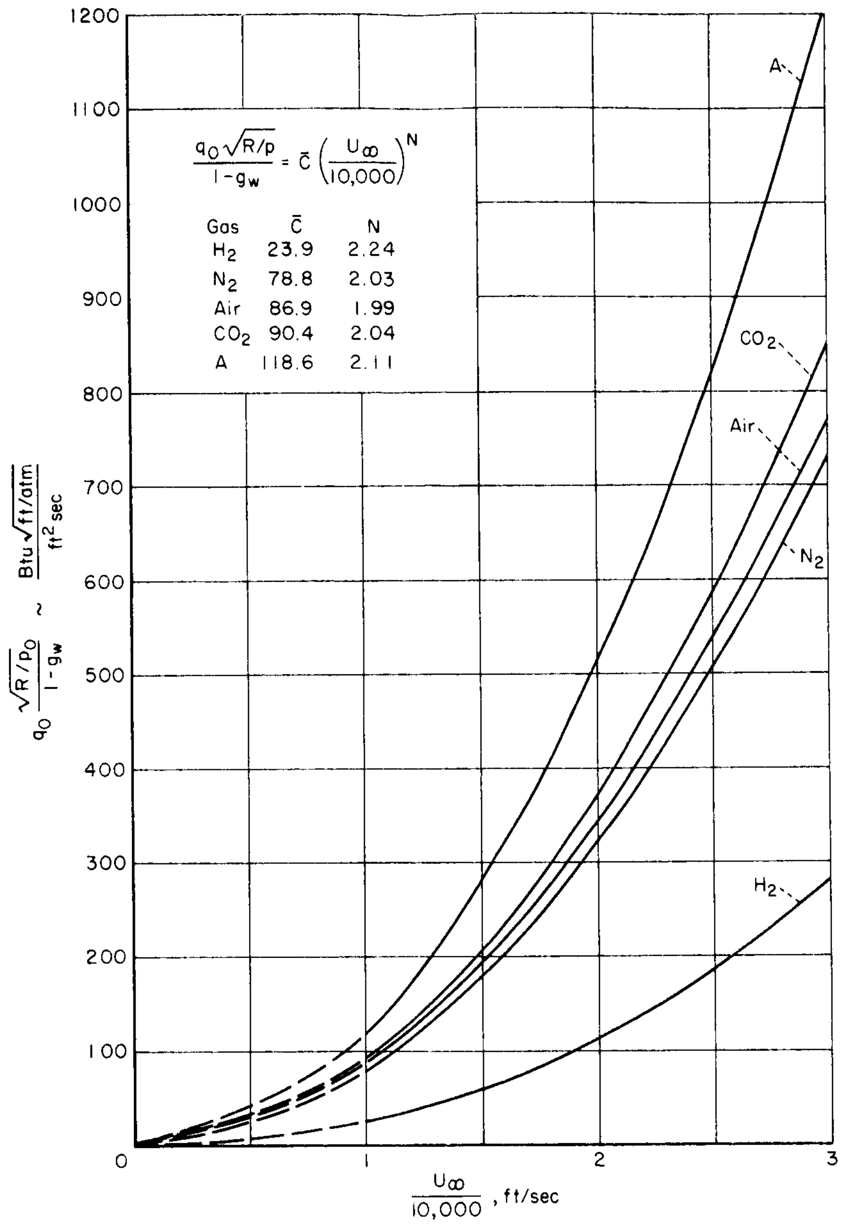

Figure 18.- Stagnation-point heat transfer for various gases.

$$\frac{q_o\sqrt{R/p_o}}{1 - g_w} = 2.64\times10^{-3}\ \frac{1}{Pr_w}\ \sqrt[4]{\frac{\left[(\rho\mu)_{T=500^\circ\ R}\right]^2}{p_o\rho_{e_o}}}\left(\frac{1 - \varphi_D}{h_D - h_w}\right)^{-0.15} U_\infty^{1.7} \tag{14}$$

where ρ is expressed in slugs/ft^3, μ in slugs/ft sec, h in ft^2/sec^2, U_∞ in ft/sec, and p_o in atm. Equation (14) can be used to estimate the heating rate in various gases. To apply the equation, knowledge of the low temperature properties of the gas along with the stagnation-point pressure and density is required.

To substantiate the theoretical predictions made above, a comparison of theory and experiment is given in figures 19(a) to (d). Here, heating-rate

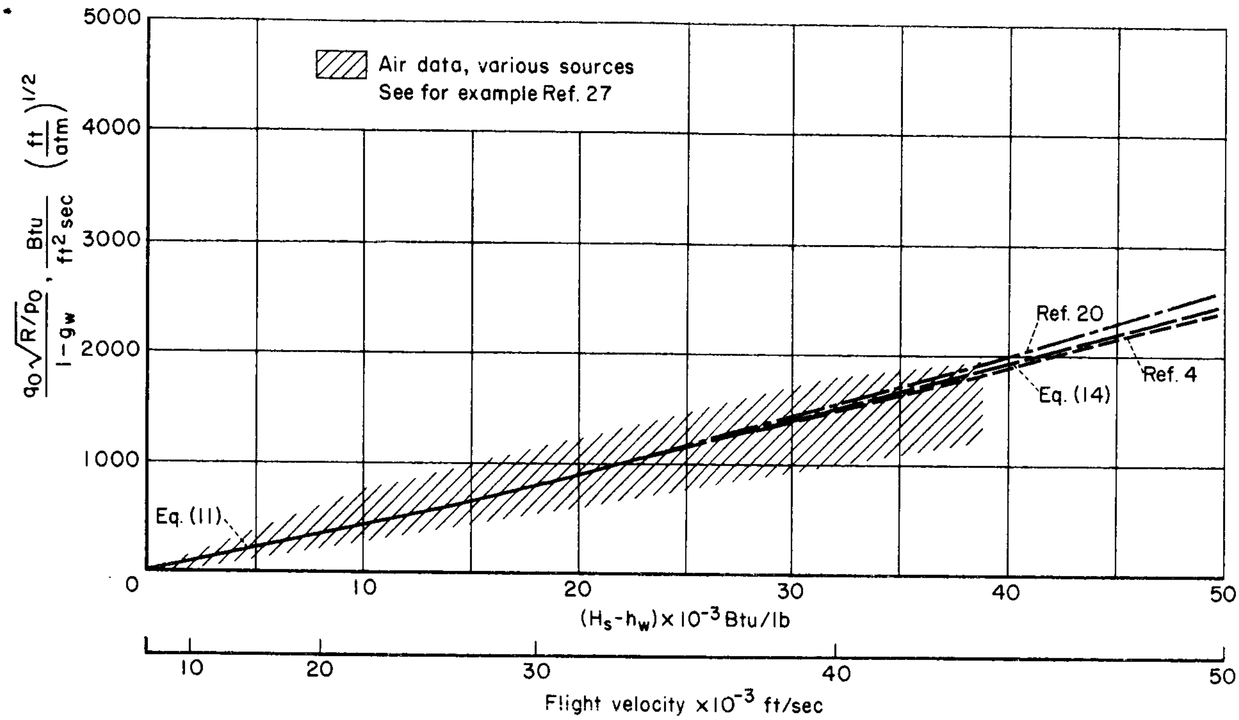

(a) Air.

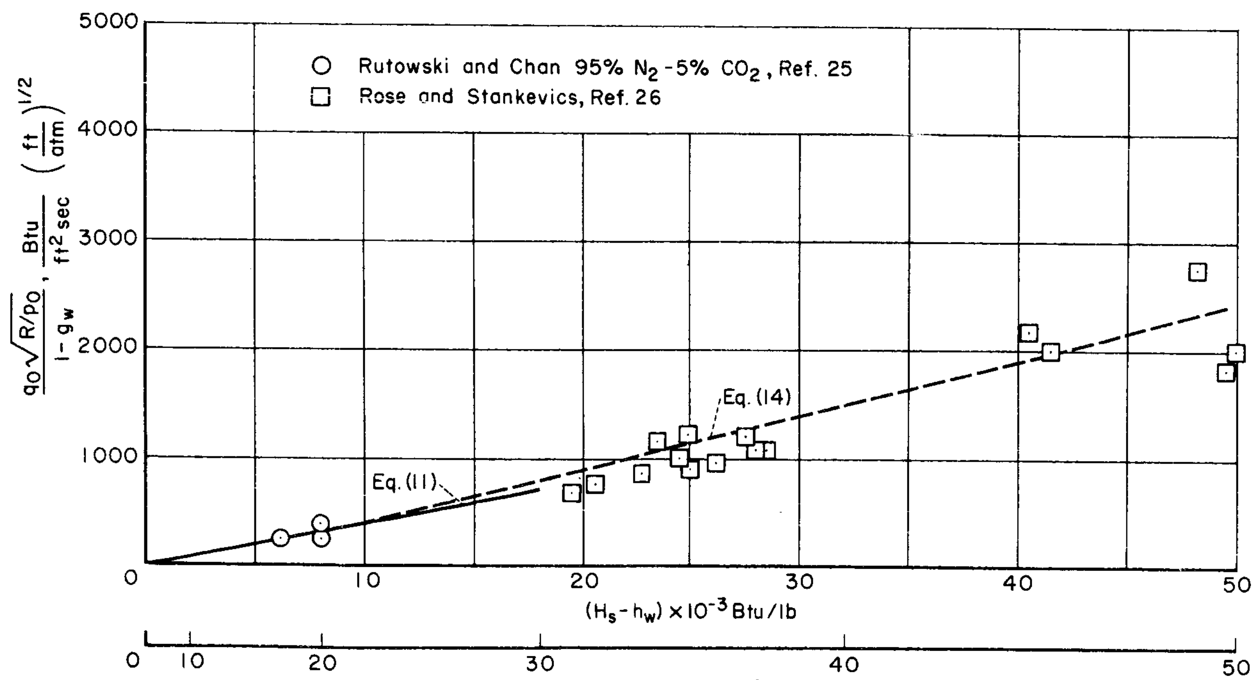

(b) Nitrogen.

Figure 19.- Comparison of theory and data.

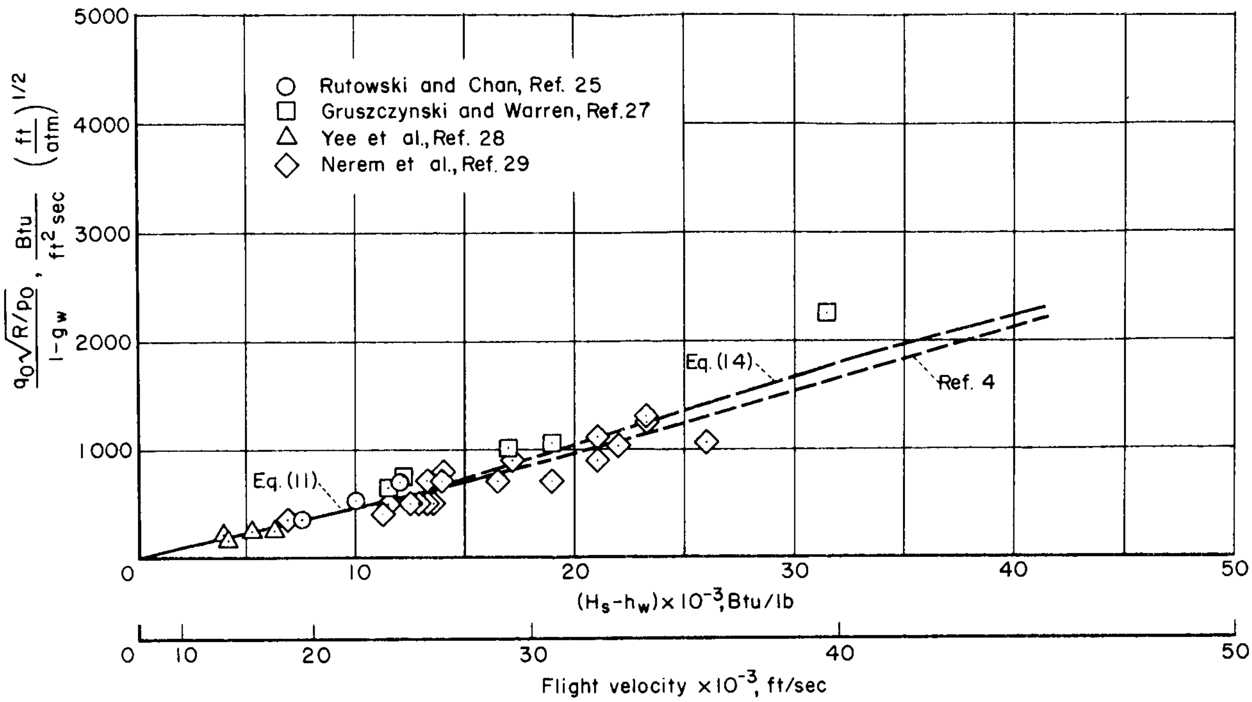

(c) Carbon dioxide.

Figure 19.- Continued.

data from various sources are plotted against $(H_s - h_w)$. For air, the shaded area represents the majority of shock-tube data from a large number of sources. The solid lines represent equation (11) with the appropriate values of $\overline{C}$ and N. The data and equation (11) agree well for all the gases. Also, equation (11) agrees very well with the theory of reference 4 for air and CO_2 and reference 20 for air.

Equation (14) is also shown in figure 19 evaluated for $p_o = 0.1$ atm. This equation, as expected, agrees well with equation (11) up to 30,000 ft/sec. To demonstrate the utility of this equation, which uses the correlation shown in figure 17, it was extrapolated to substantially higher enthalpies. The agreement with the data is good. Also, the theory of reference 20, which includes the use of the high temperature transport properties of air, and the extrapolation of equation (14) agree favorably in the extrapolated region where ionization and dissociation occur together in the boundary layer. Therefore, it appears that the heating rate in various gases can be predicted adequately to very high enthalpies by an equation based on relatively low-temperature properties.

Next, the problem of heat distribution on the surface of the body is considered.

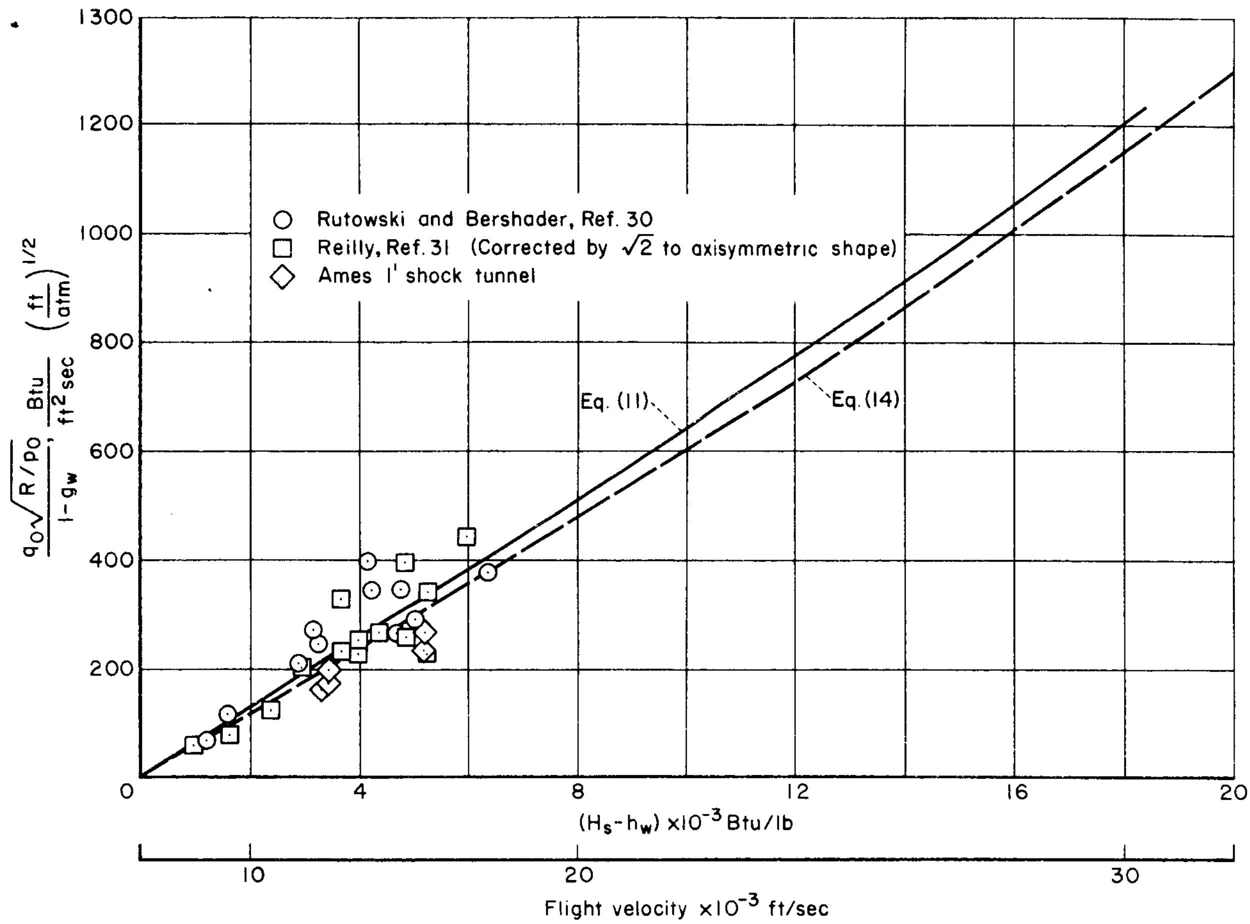

(d) Argon.

Figure 19.- Concluded.

Heating-Rate Distribution

Equation (6) shows that the distribution of heat transfer around a body depends explicitly on the inviscid flow as reflected in the boundary-layer-edge velocity and surface pressure and implicitly on the inviscid and viscid flow as reflected in the variation of $g'(o)/g_o'(o)$ with pressure gradient. An investigation of the magnitude of this ratio of enthalpy gradients is presented next and it shows that including this ratio in the heating-rate distribution equation modifies the results by a small amount.

Figure 20 presents the variation of $g'(o)/g_o'(o)$ for an axisymmetric body with pressure-gradient parameter for each of the gases for a single value of the dissipation term $u_e^2/H_s = 1/2$ at three flight velocities and at a specified wall temperature and pressure. Each gas shows an increase in this ratio with increasing pressure gradient. Positive values of β imply favorable pressure gradient. The ratio of enthalpy gradients for any particular gas varies by about 10 percent over the range of β considered. It is noteworthy

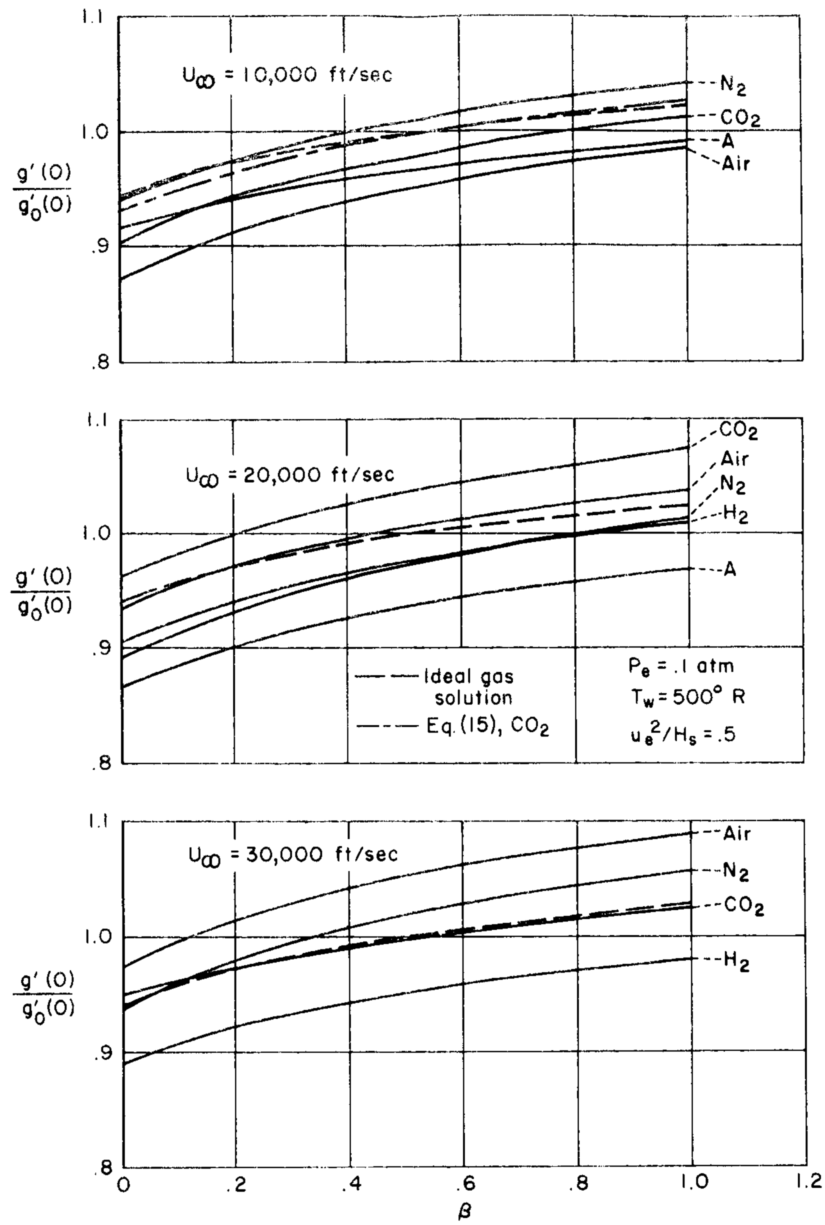

Figure 20.- Enthalpy-gradient variation with pressure-gradient parameter for axisymmetric configurations.

that the curves do not always pass through 1.0 at $\beta = 1/2$ as a direct consequence of including the dissipation term in the equations and, as pointed out before, its effect on the solution is small. For all values of the dissipation term used in this investigation, the effect never exceeded 10 percent. If the dissipation term is neglected, the correlation equations presented in figures 6 through 10 can be used to express the axisymmetric value of $g'(o)/g_o'(o)$ as

$$\frac{g'(o)}{g_o'(o)} = \frac{1 + c\sqrt{\beta}}{1 + 0.707c} \tag{15}$$

where c is the constant given in figures 6 to 10.

It is interesting to compare the variation of $g'(o)/g_o'(o)$ with that obtained in reference 21 for an ideal-gas solution to the boundary-layer equations with φ and Pr set equal to 1. The dashed curve in figure 20 represents such an ideal-gas solution, and as shown, this approximation represents quite adequately the real-gas variation. This ideal solution is also compared with equation (15) for carbon dioxide (see U_∞ = 10,000 ft/sec) and the comparison is very good. Either method for obtaining $g'(o)/g_o'(o)$ is adequate for the range of pressure-gradient parameters considered. Ideal-gas solutions to pressure-gradient parameters of 4.0 are tabulated in reference 21.

It is concluded that the transport and thermodynamic property variations play a minor role in determining the heating-rate distribution, at least for a practical range of the pressure-gradient parameter, whereas the external flow field is of major importance.

CONCLUSIONS

An investigation of the effects of gas composition on the equilibrium convective heating rate and heating-rate distribution resulted in the following conclusions:

1. The effect of the transport property variations in the higher energy portions of the boundary layer was not reflected in the wall enthalpy gradient. At large η changes by a factor of 3 in thermal conductivity or viscosity changed the wall enthalpy gradient and therefore convective heating rate less than 10 percent. For the range of parameters investigated, this indicates that precise evaluation of transport properties at high temperatures is not critical to equilibrium convective heat-transfer calculations.

2. The wall enthalpy gradient obtained from solutions to the similar form of the equilibrium boundary-layer equations for air, nitrogen, hydrogen, carbon dioxide, and argon can be correlated on low temperature properties. This correlation can be used to extend the present results to other gases and to higher total enthalpies.

3. The stagnation-point heat transfer depends on gas composition. For the same body radius, total pressure, and flight velocity, argon gives the highest heat transfer and hydrogen gives the lowest value. Air, nitrogen, and CO_2 give about the same intermediate value of heat transfer.

4. The heating-rate distribution on a body is affected to a minor degree by the gas composition. For practical application, the heating-rate distribution to blunt bodies can be obtained from inviscid flow considerations alone. Refinements to this can be obtained by using solutions to the low speed form of the boundary-layer equations.

Ames Research Center
National Aeronautics and Space Administration
Moffett Field, Calif., Feb. 23, 1965

APPENDIX A

DERIVATION AND SOLUTION OF EQUATIONS

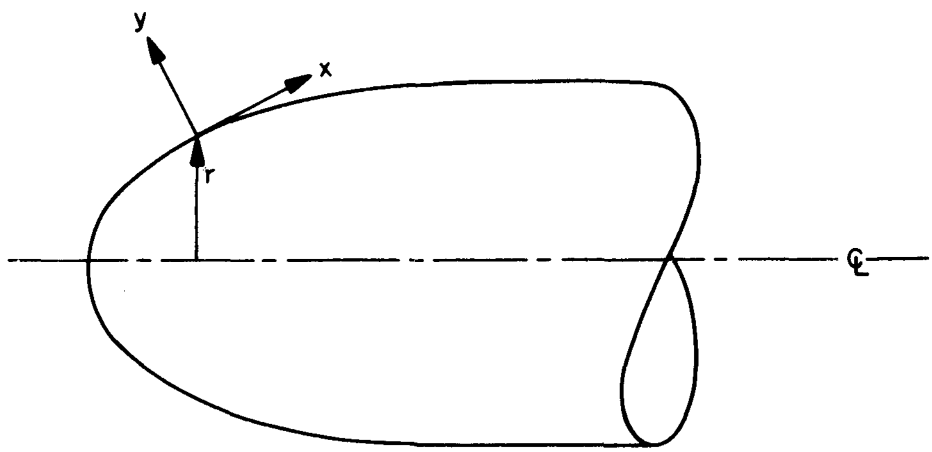

The analysis is restricted to a gas in thermochemical equilibrium whose chemically reacting species are considered a mixture of perfect gases. For such a gas, the general equations of change for a body-oriented coordinate system (see sketch above) subject to Prandtl's boundary-layer assumptions are:

$$\frac{\partial}{\partial x}\left(r^n \rho u\right) + \frac{\partial}{\partial y}\left(r^n \rho v\right) = 0 \tag{A1}$$

$$\rho u \frac{\partial u}{\partial x} + \rho v \frac{\partial u}{\partial y} + \frac{dp}{dx} - \frac{\partial}{\partial y}\left(\mu \frac{\partial u}{\partial y}\right) = 0 \tag{A2}$$

$$\rho u \frac{\partial H}{\partial x} + \rho v \frac{\partial H}{\partial y} - \frac{\partial}{\partial y}\left(\mu \frac{\partial u^2/2}{\partial y}\right) + \frac{\partial q_y}{\partial y} = 0 \tag{A3}$$

where $n = 1$ for axisymmetric bodies and $n = 0$ for two-dimensional bodies. Equation (A1) is the continuity equation and represents the sum of the individual species equations. Equation (A2) is the momentum equation which relates the momentum change to the pressure and viscous shear forces acting on the system. Equation (A3) is the energy equation which relates the enthalpy change to heat addition by viscous stresses and the normal component of the heat-flux vector, q_y.

The normal component of the heat-flux vector (neglecting thermal diffusion and radiation) is related to the temperature and molar concentration of the gas by the equation (see ref. 19)

$$q_y = -k_f \frac{\partial T}{\partial y} + \sum_i \frac{\overline{n}^2}{\rho} h_i \sum_{j \neq i} m_i m_j D_{ij} \frac{\partial X_j}{\partial y} \tag{A4}$$

The first and second terms on the right side of equation (A4) represent, respectively, heat addition due to conduction and due to diffusion of species across the boundary layer. Enthalpy is introduced into equation (A4) as follows. The molar concentration and enthalpy of the gas in equilibrium vary with temperature only (the pressure is considered constant across the boundary layer) so

$$\frac{\partial X_j}{\partial y} = \left(\frac{\partial X_j}{\partial T}\right)_p \frac{\partial T}{\partial y} \tag{A5}$$

and

$$\frac{\partial h}{\partial y} = \left(\frac{\partial h}{\partial T}\right)_p \frac{\partial T}{\partial y} \tag{A6}$$

and by definition the total specific heat is

$$\left(\frac{\partial h}{\partial T}\right)_p \equiv c_p = \sum_i c_{p_i} C_i + \sum_i h_i \frac{dC_i}{dT} \tag{A7}$$

Therefore (A4), with the aid of equations (A5) and (A6) and the above definition of specific heat, becomes

$$q_y = -\frac{1}{c_p} \left[k_f - \sum_i \frac{\overline{n}^2}{\rho} h_i \sum_{j \neq i} m_i m_j D_{ij} \frac{\partial X_j}{\partial T}\right] \frac{\partial h}{\partial y} \tag{A8a}$$

or

$$q_y = -\frac{k}{c_p} \frac{\partial h}{\partial y} \tag{A8b}$$

where the bracketed term in equation (A8a) is the so-called "total" thermal conductivity k.

Now, the energy conservation equation (eq. (A3)) is rewritten with the aid of (A8b) as

$$\rho u \frac{\partial H}{\partial x} + \rho v \frac{\partial H}{\partial y} - \frac{\partial}{\partial y}\left(\mu \frac{\partial u^2/2}{\partial y}\right) - \frac{\partial}{\partial y}\left(\frac{\mu}{Pr} \frac{\partial h}{\partial y}\right) = 0 \tag{A9}$$

where Pr represents the total Prandtl number of the gas obtained when total values of thermal conductivity and specific heat are used. Equation (A9) may be rearranged to give the energy equation

$$\rho u \frac{\partial H}{\partial x} + \rho v \frac{\partial H}{\partial y} - \frac{\partial}{\partial y}\left[\mu\left(\frac{\partial H}{\partial y} + \frac{1 - Pr}{Pr}\frac{\partial h}{\partial y}\right)\right] = 0 \tag{A10}$$

Equations (A1), (A2), and (A10) are the conservation equations for a reacting gas in thermochemical equilibrium. The solution to these equations is required when the heat flux to a wall is computed. This is apparent by inspection of equation (A8) (evaluated at the wall),

$$q_w = \frac{k_w}{c_{p_w}}\left(\frac{\partial h}{\partial y}\right)_w = \frac{\mu_w}{Pr_w}\left(\frac{\partial h}{\partial y}\right)_w \tag{A11}$$

To put equations (A1), (A2), and (A10) in a form more suitable for solution, the following transformations are introduced:

$$\xi \equiv \int_0^x \rho_w \mu_w u_e r^{2n}\, dx \tag{A12a}$$

$$\eta \equiv \frac{r^n u_e}{\sqrt{2\xi}} \int_0^y \rho\, dy \tag{A12b}$$

The transformed differential operators then become:

$$\frac{\partial(\ )}{\partial x} = \rho_w \mu_w u_e r^{2n} \frac{\partial(\ )}{\partial \xi} + \frac{\partial \eta}{\partial x}\frac{\partial(\ )}{\partial \eta} \tag{A13}$$

$$\frac{\partial(\ )}{\partial y} = \frac{r^n \rho u_e}{\sqrt{2\xi}} \frac{\partial(\ )}{\partial \eta} \tag{A14}$$

It is convenient to make the following definitions:

$$\frac{\partial f}{\partial \eta} \equiv \frac{u}{u_e}, \quad u = u_e \frac{\partial f}{\partial \eta} \tag{A15}$$

$$g \equiv \frac{H}{H_s} = \frac{h + (u^2/2)}{H_s} \tag{A16}$$

$$\varphi \equiv \frac{\rho\mu}{\rho_w \mu_w} \tag{A17}$$

$$\frac{\partial \psi}{\partial y} \equiv r\rho u \tag{A18a}$$

$$\frac{\partial \psi}{\partial x} \equiv -r\rho v \tag{A18b}$$

The continuity equation is satisfied by the introduction of the stream function ψ defined by equations (A18a) and (A18b). Applying the above definitions and the transformed differential operators results in the following form of the equations:

<u>Momentum</u>

$$(\varphi f_{\eta\eta})_\eta + f f_{\eta\eta} + \beta \left(\frac{\rho_e}{\rho} - f_\eta^{\,2}\right) = 2\xi (f_\eta f_{\eta\xi} - f_\xi f_{\eta\eta}) \tag{A19}$$

<u>Energy</u>

$$\left(\frac{\varphi}{Pr} g_\eta\right)_\eta + f g_\eta + \frac{u_e^{\,2}}{H_s}\left[\left(\varphi - \frac{\varphi}{Pr}\right) f_\eta f_{\eta\eta}\right]_\eta = 2\xi (f_\eta g_\xi - f_\xi g_\eta) \tag{A20}$$

where the subscripts denote partial differentiation with respect to that variable and

$$\beta \equiv 2\,\frac{d\,ln\,u_e}{d\,ln\,\xi} \tag{A21}$$

Equations (A19) and (A20) comprise a set of simultaneous, nonlinear partial differential equations. The local similarity assumption is used to solve this system of equations. In this approach, the terms on the right side of equations (A19) and (A20) are assumed small compared to other terms in the equations so that methods applying to solutions of ordinary differential equations can be applied. This means that changes of the dependent variable with ξ are negligible and that the quantities at the boundary-layer edge assume their local values as specified by external flow conditions. Further discussion of local similarity and its application can be found in references 1 and 3.

The similar form of transformed boundary-layer equations for the conservation of momentum and energy form a coupled pair of ordinary, nonlinear differential equations of third order in f and second order in g. These are written as

$$(\varphi f'')' + f f'' + \beta\left(\frac{\rho_e}{\rho} - f'^2\right) = 0 \tag{A22}$$

$$\left(\frac{\varphi}{Pr} g'\right)' + f g' + \frac{u_e^{\,2}}{H_s}\left[\left(\varphi - \frac{\varphi}{Pr}\right) f' f''\right]' = 0 \tag{A23}$$

where the prime denotes differentiation with respect to η, that is, $d/d\eta$. These equations comprise an initial value problem requiring five conditions at $\eta = 0$ (namely $f(o)$, $f'(o)$, $f''(o)$, $g(o)$, and $g'(o)$) for a unique solution. Since only three of these conditions are considered known, one must seek a solution using iterative techniques. This is accomplished by imposing two additional conditions on the equations as $\eta \to \infty$. The boundary conditions for the equations in this case are:

$$
\begin{aligned}
f(o) &= 0 \qquad & f'(\infty) &\to 1 \\
f'(o) &= 0 & & \\
g(o) &= g_w & g(\infty) &\to 1
\end{aligned}
$$

It is advisable to eliminate the explicit forms of the property derivatives from the equations since the accuracy of these terms would be highly questionable at high temperatures. This can be done by introducing the following integrating factor

$$I \equiv e^{\int_0^\eta \frac{f}{\varphi} d\eta} \tag{A24}$$

so that

$$\frac{dI}{d\eta} = \frac{f}{\varphi} I$$

Equation (A22) may be rewritten as

$$(\varphi f'')'I + ff''I + \beta\left(\frac{\rho_e}{\rho} - f'^2\right) I = 0$$

which when integrated from 0 to η and solved for f'' gives:

$$f'' = \frac{1}{\varphi I}\left[f''_w - \beta \int_0^\eta I\left(\frac{\rho_e}{\rho} - f'^2\right) d\eta\right] \tag{A25}$$

Equation (A23) when integrated from 0 to η and solved for g'/Pr gives

$$\frac{g'}{Pr} = \frac{1}{\varphi}\left[\left(\frac{g'}{Pr}\right)_w - fg + \int_0^\eta f'g \, d\eta + \frac{u_e^2}{H_s}\left(\frac{\varphi}{Pr} - \varphi\right) f'f''\right] \tag{A26}$$

Define

$$\alpha \equiv \int_0^\eta \frac{f}{\varphi} d\eta \tag{A27}$$

$$\delta \equiv \int_0^\eta \left(\frac{\rho_e}{\rho} - f'^2\right) e^\alpha \, d\eta \tag{A28}$$

$$\gamma \equiv \int_0^\eta f' g \, d\eta \tag{A29}$$

Then the conservation equations may be written as:

$$f'' = \frac{1}{\varphi} (f''_w - \beta\delta) e^{-\alpha} \tag{A30}$$

$$\frac{g'}{Pr} = \frac{1}{\varphi} \left[\left(\frac{g'}{Pr}\right)_w - fg + \gamma + \frac{u_e{}^2}{H_s}\left(\frac{\varphi}{Pr} - \varphi\right) f'f''\right] \tag{A31}$$

Equations (A27) through (A31) along with

$$f = \int_0^\eta f' \, d\eta \tag{A32}$$

are the six equations to be solved simultaneously to determine f''_w, g'_w, and profile distributions throughout the boundary layer.

The iterative technique that is used to obtain a solution is one of successive approximations based on the Newton-Raphson method (see ref. 22). The functions, f' and g, are expanded in a Taylor series where $\eta \to \infty$ and the higher order terms neglected. Thus, for $f'(\infty) = F(f''_w, g'_w)$ and $g(\infty) = G(f''_w, g'_w)$ we have

$$df'(\infty) = \frac{\partial f'(\infty)}{\partial f''_w} df''_w + \frac{\partial f'(\infty)}{\partial g'_w} dg'_w \tag{A33}$$

$$dg(\infty) = \frac{\partial g(\infty)}{\partial f''_w} df''_w + \frac{\partial g(\infty)}{\partial g'_w} dg'_w \tag{A34}$$

By approximating the differentials with finite differences we may obtain improved approximations for f''_w and g'_w as follows:

$$df'(\infty) = f'_o(\infty) - f'(\infty) = \frac{\partial f'(\infty)}{\partial f''_w} (f''_{w_o} - f''_w) + \frac{\partial f'(\infty)}{\partial g'_w} (g'_{w_o} - g'_w) \tag{A35}$$

$$dg(\infty) = g_o(\infty) - g(\infty) = \frac{\partial g(\infty)}{\partial f''_w} (f''_{w_o} - f''_w) + \frac{\partial g(\infty)}{\partial g'_w} (g'_{w_o} - g'_w) \tag{A36}$$

where the subscript o represents the corrected values so that $f_o'(\infty) = 1$ and $g_o'(\infty) = 1$, and we have:

$$\Delta g' = g'_{w_o} - g'_w = \frac{\frac{\partial g(\infty)}{\partial f''_w}[1 - f'(\infty)] - \frac{\partial f'(\infty)}{\partial f''_w}[1 - g(\infty)]}{\left[\frac{\partial f'(\infty)}{\partial g'_w}\right]\left[\frac{\partial g(\infty)}{\partial f''_w}\right] - \left[\frac{\partial f'(\infty)}{\partial f''_w}\right]\left[\frac{\partial g(\infty)}{\partial g'_w}\right]} \tag{A37}$$

$$\Delta f'' = f''_{w_o} - f''_w = \frac{1 - f''_w - \left[\frac{\partial f'(\infty)}{\partial g'_w}\right]\Delta g'}{\left[\frac{\partial f'(\infty)}{\partial f''_w}\right]} \tag{A38}$$

The iteration scheme is started with two initial guesses for f''_w and g'_w (denoted by f''_{w_1}, f''_{w_2}, g'_{w_1}, and g'_{w_2}) and equations (A27) through (A32) are integrated (by the Adams-Moulton numerical integration method) to sufficiently high values of η to insure $f''(\eta) \to 0$ and $g'(\eta) \to 0$ for the three combinations of initial guesses (f''_{w_1}, g'_{w_1}), (f''_{w_2}, g'_{w_1}), and (f''_{w_1}, g'_{w_2}). These three solutions give sufficient information for determining the partial derivatives in equations (A37) and (A38) by a finite difference. With the initial guesses improved by $\Delta f''$ and $\Delta g'$ the process may be repeated until the solution is converged upon to the desired accuracy. The requirements for convergence for the data in this paper were:

$$|f'(\infty) - 1| \leq 0.0005 \qquad |f''(\infty)| \leq 0.0005$$

$$|g(\infty) - 1| \leq 0.0005 \qquad |g'(\infty)| \leq 0.0005$$

This required on the average two to three cycles of the iterative process.

APPENDIX B

REAL-GAS PROPERTIES

The real-gas properties used for this report were taken from the literature (refs. 6 through 15) and were curve fitted with polynomials for use in the boundary-layer equations. The references were chosen primarily because they presented the desired properties or sufficient information to compute the properties for increments of temperature which were always equal to or less than 1000° K for pressures ranging from 10^{-4} to 10^{2} atm. This provided sufficient input data for a least-squares polynomial curve-fit method in terms of the desired function, enthalpy. The references are felt to indicate reasonable property variations with enthalpy and pressure for the enthalpy range considered here ($20 \leq h \leq 18{,}000$ Btu/lb).

The tabulated data were fitted in sections, generally by 7th degree polynomials, and a deviation from the fitted points within ±2 percent was maintained. The equations are written in the form

$$P = a_0 + a_1\left(\frac{h}{h_r}\right) + a_2\left(\frac{h}{h_r}\right)^2 + , \ . \ . \ . \ , + a_7\left(\frac{h}{h_r}\right)^7$$

where

$$P \equiv \begin{cases} \rho_r/\rho \\ \rho\mu/\rho_r\mu_r \\ \rho\mu/Pr\rho_w\mu_w \end{cases}$$

as the case may be. The coefficients a_0 through a_7 and the h/h_r range for which they are valid are given in tables II to V. The reference values (ρ_r, h_r, and μ_r) are given in table I. In general, the property curves are continuous over the complete enthalpy range but the derivatives at the points of connection of two sections are not. This is one reason the property derivatives were eliminated from the boundary-layer equations. The property curve fits for air were taken directly from reference 23.

REFERENCES

1. Lees, Lester: Laminar Heat Transfer Over Blunt-Nose Bodies at Hypersonic Flight Speeds. Jet Propulsion, vol. 26, no. 4, April 1956, pp. 259-269, 274.

2. Fay, Jay A.; and Riddell, Frank R.: Stagnation Point Heat Transfer in Dissociated Air. Res. Note 18, Avco Res. Lab., June 1956.

3. Kemp, Nelson H.; Rose, Peter H.; and Detra, Ralph W.: Laminar Heat Transfer Around Blunt Bodies in Dissociated Air. Res. Rep. 15, Avco-Everett Res. Lab., May 1958. (Also J. Aerospace Sci., vol. 26, no. 7, July 1959, pp. 421-30.)

4. Hoshizaki, H.: Heat Transfer in Planetary Atmospheres at Super-Satellite Speeds. Am. Rocket Soc. Paper 2173-61. ARS J., vol. 32, Oct. 1962, pp. 1544-51.

5. Scala, S. M.; and Gilbert, L. M.: Theory of Hypersonic Laminar Stagnation Region Heat Transfer in Dissociating Gases. R63SD40, Gen. Elec. Space Sci. Lab., April 1963.

6. Hansen, C. Frederick: Approximations for the Thermodynamic and Transport Properties of High-Temperature Air. NASA TR R-50, 1959.

7. Hilsenrath, J.; Beckett, C. W.; et al.: Tables of Thermodynamic and Transport Properties of Air, Argon, Carbon Dioxide, Carbon Monoxide, Hydrogen, Nitrogen, Oxygen and Steam. Pergamon Press, New York, Oxford, 1960.

8. Ahtye, Warren F.; and Peng, Tzy-Cheng: Approximations for the Thermodynamic and Transport Properties of High-Temperature Nitrogen With Shock-Tube Applications. NASA TN D-1303, 1962.

9. Anon.: JANAF Interim Thermochemical Tables. Vols. 1 and 2. Dow Chem. Co., Dec. 1960.

10. Kubin, Robert F.; and Presley, Leroy L.: Thermodynamic Properties and Mollier Chart for Hydrogen From 300° K to 20,000° K. NASA SP-3002, 1964.

11. Vanderslice, J. T.; Weissman, Stanley; Mason, E. A.; and Fallon, R. J.: High-Temperature Transport Properties of Dissociating Hydrogen. Phys. Fluids, vol. 5, no. 2, Feb. 1962, pp. 155-64.

12. Raymond, J. L.: Thermodynamic Properties of Carbon Dioxide to 24,000° K With Possible Application to the Atmosphere of Venus. RM 2292, Rand Corp., Nov. 26, 1958.

13. Thomas, M.: The High Temperature Transport Properties of Carbon Dioxide. Rep. SM 37790, Douglas Aircraft Co., July 1960.

14. Huseby, O. A.: Aerothermodynamic Properties of High Temperature Argon. D2-11238, Boeing Co., 1962.

15. Pindroh, A. L.: Transport Properties of Argon in Ionization Equilibrium. D2-11253, Boeing Co., 1961.

16. Cohen, Nathaniel B.: Boundary-Layer Similar Solutions and Correlation Equations for Laminar Heat-Transfer Distribution in Equilibrium Air at Velocities up to 41,100 Feet Per Second. NASA TR R-118, 1961.

17. Chapman, Gary T.: Theoretical Laminar Convective Heat Transfer and Boundary-Layer Characteristics on Cones at Speeds to 24 km/sec. NASA TN D-2463, 1964.

18. Howe, John T.; and Sheaffer, Yvonne S.: Effects of Uncertainties in the Thermal Conductivity of Air on Convective Heat Transfer for Stagnation Temperature up to 30,000° K. NASA TN D-2678, 1964.

19. Hirschfelder, Joseph O.; Curtiss, Charles F; and Bird, R. Byron: Molecular Theory of Gases and Liquids. John Wiley and Sons Inc., New York, 1954.

20. Howe, John T.; and Viegas, John R.: Solutions of the Ionized Radiating Shock Layer, Including Reabsorption and Foreign Species Effects, and Stagnation Region Heat Transfer. NASA TR R-159, 1963.

21. Beckwith, Ivan E.; and Cohen, Nathaniel B.: Application of Similar Solutions to Calculation of Laminar Heat Transfer on Bodies With Yaw and Large Pressure Gradient in High-Speed Flow. NASA TN D-625, 1961.

22. Bookston, J. M.: Notes on Iteration. GMR 157, Gen. Motors Corp., April 1958.

23. Viegas, John R.; and Howe, John T.: Thermodynamic and Transport Property Correlation Formulas for Equilibrium Air From 1,000° K to 15,000° K. NASA TN D-1429, 1962.

24. Goodwin, Glen; and Howe, John T.: Recent Developments in Mass, Momentum, and Energy Transfer at Hypervelocities. Proc. NASA-University Conference on the Science and Technology of Space Exploration, Vol. 2, NASA SP-11, 1962, pp. 291-301.

25. Rutowski, R. W.; and Chan, K. K.: Shock Tube Experiments Simulating Entry Into Planetary Atmospheres. LMSD 288139, vol. 1, pt. 2, Lockheed Missiles and Space Co., Jan. 1960.

26. Rose, P. H.; and Stankevics, J. O.: Stagnation-Point Heat-Transfer Measurements in Partially Ionized Air. AIAA, vol. 1, no. 12, Dec. 1963, pp. 2752-2763.

27. Gruszczynski, J. S.; and Warren, W. R.: Measurements of Hypervelocity Stagnation Point Heat Transfer in Simulated Planetary Atmospheres. R63SD29, Gen. Elec. Space Sci. Lab., March 1963.

28. Yee, Layton; Bailey, Harry E.; and Woodward, Henry T.: Ballistic Range Measurements of Stagnation-Point Heat Transfer in Air and Carbon Dioxide at Velocities up to 18,000 Feet Per Second. NASA TN D-777, 1961.

29. Nerem, Robert M.; Morgan, C. Joe; and Graber, Bruce C.: Hypervelocity Stagnation Point Heat Transfer in a Carbon Dioxide Atmosphere. AIAA, vol. 1, no. 9, Sept. 1963, pp. 2173-2175.

30. Rutowski, R. W.; and Bershader, D.: Shock Tube Studies of Radiative Transport in an Argon Plasma. Phys. Fluids, vol. 7, no. 4, April 1964, pp. 568-577.

31. Reilly, James P.: Stagnation Point Heating in Ionized Monatomic Gases. Publication 64-1 (AFOSR 5442), Fluid Mechanics Laboratory, Mass. Inst. of Tech., Jan. 1964.

TABLE I.- REFERENCE VALUES

Gas	Pressure level, atm	h_r, ft^2/sec^2	ρ_r, $slugs/ft^3$	$\rho_r\mu_r$, $slugs^2/ft^4\ sec$
N_2	10^{-4}	2.16×10^8	1.03982×10^{-8}	2.13804×10^{-14}
	10^{-3}	↓	$.96395\times10^{-7}$	2.08976×10^{-13}
	10^{-2}		$.88964\times10^{-6}$	2.04719×10^{-12}
	10^{-1}		$.81765\times10^{-5}$	2.00279×10^{-11}
	10^{0}		$.74780\times10^{-4}$	1.95008×10^{-10}
	10^{1}		$.68241\times10^{-3}$	1.89914×10^{-9}
	10^{2}		$.62148\times10^{-2}$	1.84316×10^{-8}
CO_2	10^{-4}		1.07882×10^{-8}	2.21260×10^{-14}
	10^{-3}		1.08852×10^{-7}	2.33707×10^{-13}
	10^{-2}		$.97016\times10^{-6}$	2.24302×10^{-12}
	10^{-1}		$.93717\times10^{-5}$	2.18242×10^{-11}
	10^{0}		$.86150\times10^{-4}$	2.20876×10^{-10}
	10^{1}		$.86926\times10^{-3}$	2.21448×10^{-9}
	10^{2}		$.81299\times10^{-2}$	2.15642×10^{-8}
A	10^{-4}		$.80467\times10^{-8}$	2.29064×10^{-14}
	10^{-3}		$.73606\times10^{-7}$	2.32691×10^{-13}
	10^{-2}		$.67143\times10^{-6}$	2.35307×10^{-12}
	10^{-1}		$.60912\times10^{-5}$	2.43368×10^{-11}
	10^{0}		$.54787\times10^{-4}$	2.53336×10^{-10}
	10^{1}		$.48696\times10^{-3}$	2.64735×10^{-9}
H_2	10^{-4}		$.34617\times10^{-8}$	1.77857×10^{-15}
	10^{-3}		$.34512\times10^{-7}$	1.77319×10^{-14}
	10^{-2}		$.34460\times10^{-6}$	1.77049×10^{-13}
	10^{-1}		$.34460\times10^{-5}$	1.77049×10^{-12}
	10^{0}		$.34460\times10^{-4}$	1.77049×10^{-11}
	10^{1}		$.34460\times10^{-3}$	1.77049×10^{-10}
	10^{2}		$.34460\times10^{-2}$	1.77049×10^{-9}

TABLE II.- PROPERTY COEFFICIENTS FOR CARBON DIOXIDE

	p, atm	h/h_r limits Lower	h/h_r limits Upper	a_0	a_1	a_2	a_3	a_4	a_5	a_6	a_7
ρ_r/ρ	.0001	.00863	.85	.5399714E-02	.2484537E 01	-.9626072E 01	.1666290E 02	-.2149784E 01	-.7599813E 01	-.1800463E 02	.2081456E 02
		.85	2.3832	-.8467210E 01	.2430804E 02	-.1936303E 02	.4109565E-00	.7065300E 01	-.3548554E 01	.6138501E 00	-.2449876E-01
	.001	.00863	.835	.2220041E-02	.2753129E 01	-.1372176E 02	.4029716E 02	-.3694833E 02	-.4601074E 02	.1019767E 03	-.4708394E 02
		.835	2.2089	-.7481494E 00	.7660741E 00	.3860829E 01	-.3862913E 01	.7236640E 00	.4470813E-00	-.1872569E-00	.1841421E-01
	.01	.00863	1.05	.3437818E-02	.2406317E 01	-.1324137E 02	.6143467E 02	-.1606372E 03	.2210408E 03	-.1488086E 03	.3882039E 02
		1.05	2.3745	-.2001904E 01	-.1403684E 01	.1090629E 02	-.6843544E 01	-.9563222E 00	.1583165E 01	-.2236096E-00	-.2723496E-01
	.1	.00862	1.05	.1358342E-02	.2220082E 01	-.7870914E 01	.1796043E 02	-.1150383E 02	-.2149262E 02	.3725500E 02	-.1554344E 02
		1.05	2.0693	-.2171585E 01	.6989399E 01	-.5386470E 01	.1706759E 01	-.5548193E 00	.8510089E 00	-.5014329E 00	.9027476E-01
	1.	.00856	.92	.2745447E-02	.1954775E 01	-.6021587E 01	.1097633E 02	-.1915656E 01	-.2035392E 02	.2594607E 02	-.9596404E 01
		.92	2.1742	-.8654817E 01	.1865795E 02	-.6726933E 01	-.5868841E 01	.2713320E 01	.2156939E 01	-.1536914E 01	.2568615E-00
	10.	.00784	1.02	.3758254E-02	.1873356E 01	-.5124505E 01	.1004912E 02	-.7245825E 01	-.3546410E 01	.8395230E 01	-.3385894E 01
		1.02	2.1562	-.4117738E 01	.8749274E 01	-.2988564E 01	-.1166755E 01	-.6762212E-01	.9993197E 00	-.4354574E-00	.5331097E-01
	100.	.01818	1.02	.9654950E-02	.1549840E 01	-.2834658E 01	.3379769E 01	.9883208E 00	-.4960785E 01	.3710885E 01	-.8398197E 00
		1.02	2.004	.2248317E 02	-.6053603E 02	.4784961E 02	.7414041E 00	-.6936493E 01	-.8774515E 01	.7737177E 01	-.1563783E 01
ϕ	.0001	.00863	.65	.5257455E 01	-.3990463E 02	.3082436E 03	-.1437796E 04	.3842238E 04	-.5862093E 04	.4804434E 04	-.1656314E 04
		.65	2.3832	.3059479E 01	-.1125013E 01	-.4749493E 01	.3999087E 01	.2395782E 01	-.4010387E 01	.1658628E 01	-.2284599E-00
	.001	.00863	.5566	.4923880E 01	-.3313713E 02	.1898553E 03	-.4734219E 03	-.1898570E 03	.3057988E 04	-.5130921E 04	.2728716E 04
		.5566	2.2089	.1329750E 01	.2239477E 01	-.5648478E 01	.3164205E 01	.9525569E 00	-.1533995E 01	.5387136E 00	-.6533159E-01
	.01	.00863	.5685	.5116525E 01	-.3463982E 02	.2209541E 03	-.8369217E 03	.1602072E 04	-.1139826E 04	-.4359274E 03	.7028398E 03
		.5685	2.3745	.1831134E 01	.1434352E 01	-.5762816E 01	.3995655E 01	.3833830E-00	-.1347489E 01	.4799735E-00	-.5192355E-01
	.1	.00862	.6155	.5227716E 01	-.3270751E 02	.1644435E 03	-.3611363E 03	-.1488730E 03	.1980218E 04	-.3044459E 04	.1500282E 04
		.6155	2.0693	.2973215E 01	-.4137632E 01	.4654700E 01	-.5693241E 01	.5352270E 01	-.2742240E 01	.6512987E 00	-.5176090E-01
	1.	.00856	.57	.5528567E 01	-.4101253E 02	.2911687E 03	-.1231038E 04	.2892921E 04	-.3662669E 04	.2242269E 04	-.4678437E 03
		.57	2.1742	.2715178E 01	-.2012728E 01	-.1117327E 01	.2067068E 01	-.2116347E-00	-.7275593E 00	.3756569E-00	-.5746989E-01
	10.	.00784	.5743	.5862625E 01	-.5383130E 02	.3945385E 03	-.1585123E 04	.3349647E 04	-.3391862E 04	.1034989E 04	.3391843E 03
		.5743	2.1562	.3187718E 01	-.4680280E 01	.3128793E 01	-.2409258E-00	-.6843714E 00	.2768699E-00	-.9331481E-02	-.7998673E-02
	100.	.01818	.556	-.5469334E 01	-.3984140E 02	.2685072E 03	-.1143553E 04	.2970565E 04	-.4634688E 04	.3997302E 04	-.1460812E 04
		.556	2.004	.2915289E 01	-.3396159E 01	.1367831E 01	.4454135E-00	-.4626448E-00	.1615416E-00	-.5369810E-01	.9547417E-02
ϕ/P_r	.0001	.01998	.09	.7038676E 01	-.2158073E 02	-.3886909E 03	.2569243E 04				
		.09	.829	-.8643200E 00	.8030885E 02	-.4010550E 03	.1066407E 04	-.8562820E 03	-.1537822E 04	.3222416E 04	-.1616818E 04
		.829	.85292	.2313672E 01	-.3880496E 03	.1294181E 04	.3824606E 03	-.1702918E 04	-.8952913E 03	-.4841776E 03	.1955136E 04
		.85292	2.3832	.1477012E 01	-.5998113E 01	.9918424E 01	-.6053194E 01	-.8277099E 00	.3450827E 01	-.1717502E 01	.2652143E-00
	.001	.01998	.1601	.8154074E 01	-.1776025E 03	.5353081E 04	-.8375621E 05	.3473383E 06	.3919753E 07	-.4032891E 08	.1002269E 09
		.1601	.80481	.1054000E 02	-.5340172E 02	.1578263E 03	-.3323529E 03	.4974644E 03	-.4745207E 03	.2264356E 03	-.2357980E 02
		.80481	.85	.4887583E 03	-.8264723E 03	.7693051E 02	-.1722042E 04	.2584625E 03	.3984070E 04	.2228642E 04	-.4724853E 04
		.85	.962	.3745746E 03	-.7177921E 03	.3438588E 03					
		.962	2.2089	.1912953E 02	-.3605559E 02	.2451233E 02	-.6191590E 01	.2668335E 01	-.3586010E 01	.1792502E 01	-.2918928E-00
	.01	.01998	.1352	.9830642E 01	-.3032766E 03	.8054276E 04	-.5154115E 05	-.1617371E 07	.3178230E 08	-.2071325E 09	.4676795E 09
		.1352	.8478	.1409592E 02	-.1043138E 03	.3281294E 03	-.9240307E 02	-.1847917E 04	.4484160E 04	-.4244451E 04	.1480607E 04
		.8478	1.06	.1019873E 03	.1419570E 02	-.2338231E 03	-.2431244E 02	-.2587013E 03	.1030815E 04	-.8172712E 03	.1875525E 03
		1.06	2.3745	-.2598882E 02	.6222477E 02	-.4804500E 02	.1426160E 02	-.5685539E 01	.6874681E 01	-.3406770E 01	.5445970E 00
	.1	.01998	.84018	.7711387E 01	-.6356610E 02	.4427550E 03	-.1478210E 04	.2309103E 04	-.1366307E 04	-.2653975E 03	.4245854E 03
		.84018	.9	.3508946E 02	-.2063396E 03	.1710045E-00	.2973873E 03	-.1904411E 03	.2334680E 03	.2495172E 03	-.4335941E 03
		.9	1.15	-.1004129E 04	.2038340E 04	-.2059758E 03	-.8151226E 03	-.8877050E 03	.3107983E 03	.1177077E 04	-.6096127E 03
		1.15	2.0693	.1384675E 02	-.2017318E 02	.9348815E 01	-.2196701E 01	.1736845E 01	-.2212946E-00	-.5379208E 00	.1663197E-00
	1.	.01996	.1188	.1042621E 02	-.3247322E 03	.9635617E 04	-.1292612E 06	.1494754E 06	.1504850E 08	-.1527713E 09	.4682739E 09
		.1188	.9	.2108381E 01	.2469809E 02	-.9899311E 02	.1305889E 03	-.1434034E 02	-.1378732E 03	.1307273E 03	-.3310939E 02
		.9	2.1742	.3662502E 02	-.8793670E 02	.5474137E 02	.3521432E 02	-.6013686E 02	.2805629E 02	-.5045733E 01	.2113934E-00
	10.	.01982	.1162	.7053024E 01	-.3403007E 02	-.1619871E 04	.1995362E 06	-.7321506E 07	.1182178E 09	-.8775001E 09	.2447288E 10
		.1162	.9776	.4848864E-00	.5061512E 02	-.2492428E 03	.5233382E 03	-.5102903E 03	.1253679E 03	.1311364E 03	-.6955756E 02
		.9776	2.1562	-.5829210E 02	.1352075E 03	-.6482296E 02	-.4714509E 02	.3755559E 02	.8662770E 01	-.1182147E 02	.2373911E 01
	100.	.01818	.15	.9757424E 01	-.3193224E 03	.9095704E 04	-.1064728E 06	.2168953E 06	.4875584E 07	-.3560932E 08	.7176727E 08
		.15	1.05	.3724349E 01	.1159959E 02	-.2468714E 02	-.2460468E 03	.9981355E 03	-.1470014E 04	.9564933E 03	-.2271907E 03
		1.05	2.004	.1198649E 02	-.1128825E 01	-.2325925E 02	.1680071E 02	.2628291E 01	-.4746388E 01	.6965728E 00	.1222047E-00

TABLE III.- PROPERTY COEFFICIENTS FOR NITROGEN

	p,atm	h/h_r limits Lower	h/h_r limits Upper	a_0	a_1	a_2	a_3	a_4	a_5	a_6	a_7
ρ_r/ρ	.0001	.01	.4	-.7430990E-02	.4012459E 01	-.3543739E 02	.4633788E 03	-.3193510E 04	.1142344E 05	-.2055028E 05	.1468079E 05
		.39971	2.0674	.4569639E-00	.6904414E 00	-.4038542E-00	.3247717E-00	-.1000054E-02	-.9070163E-01	.2043666E-01	.3321429E-02
	.001	.01	.4	-.7045276E-02	.3458964E 01	-.1566282E 02	.8361337E 02	.4741804E 02	-.2035760E 04	.6257247E 04	-.5817233E 04
		.4	2.091	.2604503E-00	.1709812E 01	-.2276307E 01	.1611971E 01	.1485750E-00	-.7625102E 00	.3553848E-00	-.5128022E-01
	.01	.00516	.3571	-.2920858E-02	.2976154E 01	-.1203616E 02	.1034110E 03	-.5626005E 03	.1908522E 04	-.3914418E 04	.3486680E 04
		.3571	2.0766	.2446018E-00	.1410936E 01	-.4751129E-00	-.2529212E 01	.5041291E 01	-.3901304E 01	.1394270E 01	-.1902890E-00
	.1	.00515	.3411	-.5087849E-03	.2466606E 01	-.2525627E 01	-.1325118E 02	.1165760E 03	-.1588272E 01	-.1493021E 04	.2530868E 04
		.3411	2.0	.1813536E-00	.1712794E 01	-.1651077E 01	.3215512E-00	.1373903E 01	-.1413897E 01	.5518988E 00	-.7822488E-01
	1.	.00508	.4	-.1066580E-02	.2329586E 01	-.4602642E 01	.1582396E 02	-.3537685E 02	.1892932E 03	-.7680064E 03	.9367090E 03
		.4	2.0418	-.1443560E-00	.3727302E 01	-.6816566E 01	.7113183E 01	-.3418513E 01	.3242293E-00	.2876137E-00	-.7348208E-01
	10.	.00676	.355	-.9125162E-03	.2108857E 01	-.3581981E 01	.5768007E 01	.3042635E 02	-.9415459E 02	-.6697388E 02	.2606395E 03
		.355	2.0014	.4134261E-01	.2080743E 01	-.2195262E 01	.1191887E 01	.2555831E-00	-.5880823E 00	.2489410E-00	-.3541497E-01
	100.	.00783	.3526	.8228346E-03	.1828492E 01	-.1772766E 01	-.3675546E 01	.4314267E 02	-.5789776E 02	-.1537484E 03	.2931806E 03
		.3526	2.0	-.5132102E-01	.2268186E 01	-.2208134E 01	.8998985E 00	.5696794E 00	-.6950018E 00	.2453863E-00	-.2958063E-01
ϕ	.0001	.01	.35	.4898917E 01	-.8421275E 02	.1131022E 04	-.8749392E 04	.3794234E 05	-.8807303E 05	.9542459E 05	-.3067371E 05
		.35	2.0674	.1768166E 01	-.1677893E 01	.1449019E 01	-.3014116E-00	-.6794297E 00	.6241947E 00	-.2087863E-00	.2494907E-01
	.001	.01	.2	.5039287E 01	-.8906356E 02	.1287177E 04	-.1184663E 05	.7410258E 05	-.3276646E 06	.9192425E 06	-.1164048E 07
		.2	2.091	.1689124E 01	-.9459500E 00	-.8388910E 00	.3042570E 01	-.3235814E 01	.1667472E 01	-.4193969E-00	.4075457E-01
	.01	.01	.2907	.5088503E 01	-.8369009E 02	.1024044E 04	-.6670106E 04	.2033400E 05	-.1315435E 05	-.6170000E 05	.9862870E 05
		.2907	2.0766	.1995231E 01	-.3078239E 01	.4746869E 01	-.4081570E 01	.1442998E 01	.1986324E-00	-.2764115E-00	.5320794E-01
	.1	.01	.3326	.5190075E 01	-.8487089E 02	.1053011E 04	-.7394213E 04	.2889137E 05	-.6068579E 05	.6090709E 05	-.2005734E 05
		.3326	2.0	.1906328E 01	-.2321901E 01	.2477366E 01	-.8892181E 00	-.8427823E 00	.9990482E 00	-.3806564E-00	.5140745E-01
	1.	.00508	.2946	.5379162E 01	-.9007134E 02	.1111838E 04	-.7163694E 04	.2028069E 05	-.1506771E 04	-.1050710E 06	.1481047E 06
		.2946	2.0418	.2002379E 01	-.2641410E 01	.2466279E 01	.3570218E-00	-.2850119E 01	.2411589E 01	-.8573489E 00	.1143351E-00
	10.	.01	.28984	.5493567E 01	-.9145778E 02	.1149187E 04	-.7853287E 04	.2644474E 05	-.2864835E 05	-.4846706E 05	.1039934E 06
		.28984	2.0014	.2433632E 01	-.5560292E 01	.1044111E 02	-.1106197E 02	.6388419E 01	-.1806422E 01	.1483739E-00	.1799541E-01
	100.	.01	.2785	.6107719E 01	-.1452241E 03	.2990111E 04	-.3659866E 05	.2571346E 06	-.1015459E 07	.2090158E 07	-.1741672E 07
		.2785	2.0	.2290231E 01	-.3639630E 01	.3295568E 01	.6354771E 00	-.3292227E 01	.2297358E 01	-.6483477E 00	.6388303E-01
ϕ/Pr	.0001	.01518	.3	.6870961E 01	-.1453295E 03	.2920242E 04	-.4050142E 05	.3447787E 06	-.1672723E 07	.4211019E 07	-.4242363E 07
		.3	2.0764	.3925471E 01	-.6375895E 01	.7530554E 01	-.3498827E 01	-.3151092E 01	.4625773E 01	-.2024911E 01	.3083775E-00
	.001	.01	.2181	.6792082E 01	-.1119360E 03	.1252156E 04	-.6309674E 04	.8707153E 03	.1180994E 06	-.4179868E 06	.4461278E 06
		.2181	.5	.8132172E 00	.9829951E 01	-.1493963E 02	.1373614E 01				
		.5	2.091	.3948477E 01	-.5355315E 01	.4224927E 01	-.1033416E 01	-.1173669E 01	.1010173E 01	-.2786253E-00	.2495034E-01
	.01	.01	.3	.6998676E 01	-.1215905E 03	.1553803E 04	-.1119667E 05	.4361101E 05	-.8479623E 05	.6862839E 05	-.1315946E 05
		.3	2.0766	.2290200E 01	.2927677E 01	-.1168871E 02	.1350473E 02	-.6908988E 01	.9652547E 00	.4081362E-00	-.1181444E-00
	.1	.01	.35	.7007089E 01	-.1089479E 03	.1103733E 04	-.4693645E 04	-.3255309E 04	.9430073E 05	-.2830760E 06	.2695944E 06
		.35	2.0	.2903397E 01	-.1335673E 01	-.1017667E 01	.1686001E 01	-.1536033E 01	.1056749E 01	-.4049493E-00	.6086394E-01
	1.	.00508	.4	.6945624E 01	-.1012818E 03	.1070618E 04	-.6451138E 04	.2141685E 05	-.3612444E 05	.2465845E 05	-.1185533E 04
		.4	2.0418	-.7040894E 01	.6392075E 02	-.1689922E 03	.2223978E 03	-.1610679E 03	.6391335E 02	-.1259054E 02	.8941650E 00
	10.	.01	.45	.7647384E 01	-.1363188E 03	.1704481E 04	-.1150151E 05	.4158111E 05	-.7786425E 05	.6631150E 05	-.1606769E 05
		.45	2.0014	.2520651E 01	-.2536539E-00	-.4783946E-00	-.2293820E 01	.3367748E 01	-.1645874E 01	.2833278E-00	-.2069163E-02
	100.	.01451	.4571	.7905497E 01	-.1215068E 03	.1116466E 04	-.4279618E 04	.2226147E 03	.4382779E 05	-.1124127E 06	.8785761E 05
		.4571	2.2865	.1579605E 01	.3780441E 01	-.7478124E 01	.3681068E 01	.1634484E 01	-.2480890E 01	.9748729E 00	-.1323979E-00

TABLE IV. - PROPERTY COEFFICIENTS FOR HYDROGEN

	p, atm	h/h_r limits Lower	h/h_r limits Upper	a_0	a_1	a_2	a_3	a_4	a_5	a_6	a_7
P_r/P	.0001	.04	2.4235	-.1812886E-01	.1579449E 01	-.3496316E 01	.8374563E 01	-.9619880E 01	.5669833E 01	-.1688546E 01	.2017277E-00
	.001	.01	2.682	-.8384309E-03	.1090857E 01	-.4762141E-00	.9031498E 00	-.6585025E 00	.1208427E-00	.2719739E-01	-.8018376E-02
	.01	.01	2.745	.5422658E-02	.9516558E 00	.2730678E-00	-.7074098E 00	.9571354E 00	-.6708818E 00	.2113251E-00	-.2414752E-01
	.1	.01	2.116	.3252048E-02	.9830301E 00	.4631010E-01	.4047242E-01	-.2209076E-00	.2428781E-00	-.1216749E-00	.2188060E-01
	1.	.01	2.2163	.4143644E-02	.9601897E 00	.1675240E-00	-.2182699E-00	.6839281E-01	.4746355E-01	-.4358543E-01	.8819837E-02
	10.	.01	2.0628	.3296993E-02	.9834137E 00	.3188336E-01	.8691808E-01	-.2431681E-00	.1884907E-00	-.6381368E-01	.7809189E-02
	100.	.01	2.014	.3517026E-02	.9768040E 00	.8217588E-01	-.7772721E-01	.2435920E-01	-.3479980E-01	.2697120E-01	-.6201565E-02
ϕ	.0001	.01	1.5365	.2260526E 01	-.3446737E 01	.3592214E 01	-.1142937E 01	-.7361855E 00	.5727397E 00	-.9498648E-01	.2891565E-02
	.001	.01	2.0	.2269445E 01	-.3575765E 01	.4170497E 01	-.1799110E 01	-.1072982E 01	.1539876E 01	-.6076002E 00	.7925356E-01
	.01	.01	2.0	.2274494E 01	-.3598426E 01	.4302293E 01	-.2218960E 01	-.4518944E-00	.1122043E 01	-.4980229E-00	.7440885E-01
	.1	.01	2.116	.2274215E 01	-.3597678E 01	.4383863E 01	-.2666996E 01	.4293375E-00	.3238976E-00	-.1604220E-00	.2039460E-01
	1.	.01	2.2163	.2271292E 01	-.3523100E 01	.3948120E 01	-.1606573E 01	-.8747754E 00	.1181872E 01	-.4493208E-00	.5951471E-01
	10.	.01	2.0628	.2270592E 01	-.3516871E 01	.3891643E 01	-.1409203E 01	-.1170857E 01	.1395063E 01	-.5220804E 00	.6892668E-01
	100.	.01	2.21	.2270518E 01	-.3517472E 01	.3909764E 01	-.1477533E 01	-.1070879E 01	.1327282E 01	-.5011380E 00	.6660710E-01
ϕ/P_r	.0001	.01	1.5365	.4883080E 01	-.2413394E 02	.8324159E 02	-.1356450E 03	.8305343E 02	.2196479E 02	-.4538322E 02	.1364005E 02
	.001	.01	2.0	.2789128E 01	-.2721116E 01	.5416089E 01	-.1306646E 02	.1795801E 02	-.1306552E 02	.5042712E 01	-.8262457E 00
	.01	.01	2.0	.2774841E 01	-.2177377E 01	.1899096E 01	-.3786400E 01	.5668773E 01	-.4229943E 01	.1617750E 01	-.2565491E-00
	.1	.01	2.116	.2783292E 01	-.2419752E 01	.3513700E 01	-.8349941E 01	.1212995E 02	-.8911473E 01	.3231400E 01	-.4622354E-00
	1.	.01	2.2163	.2770055E 01	-.2028002E 01	.9745715E 00	-.1867971E 01	.4058197E 01	-.3599875E 01	.1424446E 01	-.2105485E-00
	10.	.01	2.0628	.2760378E 01	-.1817348E 01	-.8886873E-02	-.2494902E-00	.3147798E 01	-.3713945E 01	.1677739E 01	-.2695168E-00
	100.	.01	2.21	.2760835E 01	-.1818611E 01	-.1082485E-00	.3076645E-00	.2013303E 01	-.2623234E 01	.1177190E 01	-.1825131E-00

TABLE V.- PROPERTY COEFFICIENTS FOR ARGON

	p, atm	h/h_r limits Lower	h/h_r limits Upper	a_0	a_1	a_2	a_3	a_4	a_5	a_6	a_7
ρ_r/ρ	.0001	.00777	.23	-.1674383E-02	.3517035E 01	-.9627985E 01	.1934744E 03	-.2349529E 04	.1826075E 05	-.7853974E 05	.1292058E 06
		.23	2.5155	.4003627E-00	.1036048E 01	-.7202238E 00	.2906399E-00	-.5947402E-01	.1266098E-00	-.9459107E-01	.1968817E-01
	.001	.00777	.23	.4720736E-03	.2934618E 01	.2967817E 01	-.3306348E 02	-.2597423E 03	.7203173E 04	-.4395595E 05	.8081579E 05
		.23	2.5115	.3871173E-00	.9785420E 00	-.3527307E-00	-.5617876E 00	.9934443E 00	-.5788796E 00	.1447469E-00	-.1237693E-01
	.01	.00777	.241	.7625674E-03	.2630952E 01	.4797006E 01	-.8121668E 02	.5234344E 03	-.5337786E 02	-.1067725E 05	.2479166E 05
		.241	2.5679	.3221987E-00	.1276558E 01	-.9247542E 00	-.6689550E-01	.8706497E 00	-.6570195E 00	.1984380E-00	-.2146588E-01
	.1	.00777	.2769	.7108967E-03	.2383391E 01	.4465835E 01	-.7616775E 02	.5554038E 03	-.1322314E 04	-.1970150E 04	.7864787E 04
		.2769	2.5794	.1596956E 00	.2436913E 01	-.4407836E 01	.5302217E 01	-.3675590E 01	.1476241E 01	-.3199241E 00	.2922252E-01
	1.	.00777	.315	-.2148519E-02	.2492387E 01	-.8462105E 01	.1202778E 03	-.8722675E 03	.3544427E 04	-.7994160E 04	.7483103E 04
		.315	2.1626	.2756052E-00	.1255176E 01	-.6136917E 00	-.6138002E 00	.1416378E 01	-.9947496E 00	.3145586E-00	-.3791633E-01
	10.	.01	.335	-.1684874E-03	.2002962E 01	-.8553262E 00	.2496850E 02	-.2914688E 03	.1649605E 04	-.4540062E 04	.4651244E 04
		.335	1.2078	.7845424E 00	-.3826235E 01	.1704210E 02	-.2742195E 02	.1435228E 02	.9432562E 01	-.1355628E 02	.4185575E 01
ϕ	.0001	.01	.195	.7557540E 01	-.1740456E 03	.2929869E 04	-.2527952E 05	.8851452E 05	.1024743E 06	-.1475926E 07	.2703059E 07
		.195	2.5155	.2872572E 01	-.3535139E 01	.2969858E 01	-.1714262E 01	.2683909E-00	.2631123E-00	-.1441926E-00	.2167485E-01
	.001	.01	.198	.7498311E 01	-.1711949E 03	.2622562E 04	-.1580945E 05	-.3917057E 05	.9562235E 06	-.4254801E 07	.6211638E 07
		.198	2.5115	.2755068E 01	-.2920364E 01	.8974454E 00	.2004859E 01	-.3243198E 01	.2044760E 01	-.6041497E 00	.6905301E-01
	.01	.01	.171	.8355741E 01	-.3001772E 03	.8514562E 04	-.1385341E 06	.1290874E 07	-.6795724E 07	.1874107E 08	-.2098974E 08
		.171	2.5679	.2754555E 01	-.3312599E 01	.2211962E 01	.3103925E-00	-.2185576E 01	.1733567E 01	-.5722290E 00	.6995222E-01
	.1	.01	.18305	.7612807E 01	-.2282979E 03	.5563463E 04	-.8088943E 05	.6946137E 06	-.3441816E 07	.9059878E 07	-.9776314E 07
		.18305	2.5794	.2691710E 01	-.3771808E 01	.4469854E 01	-.3966014E 01	.2050930E 01	-.5556612E 00	.6161858E-01	-.2347652E-03
	1.	.01	.225	.7434860E 01	-.2346580E 03	.5974720E 04	-.8986044E 05	.7930617E 06	-.4027554E 07	.1086432E 08	-.1203187E 08
		.225	2.1626	.2460788E 01	-.2472145E 01	-.1905512E-00	.5321777E 01	-.7957798E 01	.5351674E 01	-.1733866E 01	.2193666E-00
	10.	.01	.197	.6369812E 01	-.1178461E 03	.7114391E 03	.2211481E 05	-.4601071E 06	.3548122E 07	-.1250016E 08	.1675766E 08
		.197	1.25	.2887799E 01	-.7306470E 01	.1344118E 02	-.1869883E 01	-.3378481E 02	.5238827E 02	-.3175211E 02	.7011613E 01
ϕ/P_r	.0001	.01	.11659	.1251572E 02	-.4193092E 03	.1142418E 05	-.1776915E 06	.1414312E 07	-.3526070E 07	-.1893417E 08	.9873088E 08
		.11659	.25	-.2908161E 02	.1200746E 04	-.1649875E 05	.1073549E 06	-.3202905E 06	.2318381E 06	.7667239E 06	-.1226657E 07
		.25	2.2005	.6050324E 01	-.4989433E 01	.2134563E 01	-.1434250E 01	.2058690E 01	-.1655933E 01	.6093874E 00	-.8437471E-01
	.001	.01	.11658	.1229908E 02	-.4065372E 03	.1062236E 05	-.1466654E 06	.7395503E 06	.4503450E 07	-.6764986E 08	.2163506E 09
		.11658	.3	.1694992E 02	-.2789202E 03	.1950995E 04	-.4233656E 04	-.4196504E 04	.1779687E 05	.1708748E 05	-.5315014E 05
		.3	2.1637	.6001279E 01	-.4908254E 01	.1596332E 01	.1313248E-00	.1750031E-00	-.5001246E 00	.2553370E-00	-.4124090E-01
	.01	.01	.11657	.1202793E 02	-.3802375E 03	.9346736E 04	-.1188939E 06	.4965492E 06	.4364188E 07	-.5362557E 08	.1588423E 09
		.11657	.2904	.8200938E 01	-.4918000E 01	-.1281503E 04	.1363654E 05	-.5072940E 05	.5757585E 05	.5896428E 05	-.1230760E 06
		.2904	2.2408	.5944099E 01	-.4436662E 01	.3983520E-00	.1495434E 01	-.5793166E 00	-.3169567E-00	.2476729E-00	-.4350916E-01
	.1	.01	.14251	.1157175E 02	-.3586061E 03	.8653024E 04	-.1124302E 06	.6493573E 06	.2084288E 06	-.1850391E 08	.5667480E 08
		.14251	.27687	.1212984E 02	-.1193807E 03	.3019458E 03	.8302183E 03	.6998051E 04	-.7735274E 05	.1990075E 06	-.1600536E 06
		.27687	2.1855	.6022066E 01	-.5256856E 01	.3632884E 01	-.5169546E 01	.6874216E 01	-.4854028E 01	.1660967E 01	-.2196714E-00
	1.	.01	.14249	.1112380E 02	-.3462280E 03	.8438701E 04	-.1122392E 06	.6985710E 06	-.5170118E 06	-.1424302E 08	.4744618E 08
		.14249	.34524	.2942374E 01	.9052825E 02	-.1434720E 04	.7249780E 04	-.6053425E 04	-.4894866E 05	.1341178E 06	-.9903136E 05
		.34524	2.1626	.6187899E 01	-.4597021E 01	.2477518E-00	.1224415E 01	.4936576E-00	-.1311489E 01	.6329624E 00	-.9828881E-01
	10.	.01	.15544	.1048458E 02	-.3057428E 03	.6723848E 04	-.7578833E 05	.3215344E 06	.1048046E 07	-.1366236E 08	.3295877E 08
		.15544	.39405	.1128733E 02	-.9066074E 02	.1826744E 03	.2292175E 01	.7031725E 04	-.3978774E 05	.7408269E 05	-.4606336E 05
		.39405	1.25	-.6055153E 01	.8261947E 02	-.2190639E 03	.2373171E 03	-.5966081E 02	-.8387877E 02	.6487079E 02	-.1288071E 02

NASA-Langley, 1965 A-1079